

Microwave Power Control Strategies on the Drying Process

By

Wei Min Cheng

Department of Bioresource Engineering

McGill University, Montreal

June 2004

**A thesis submitted to McGill University in partial fulfillment of the
requirements for the degree of Master of Science**

©Wei Min Cheng, 2004



Library and
Archives Canada

Bibliothèque et
Archives Canada

Published Heritage
Branch

Direction du
Patrimoine de l'édition

395 Wellington Street
Ottawa ON K1A 0N4
Canada

395, rue Wellington
Ottawa ON K1A 0N4
Canada

Your file *Votre référence*

ISBN: 0-494-06381-5

Our file *Notre référence*

ISBN: 0-494-06381-5

NOTICE:

The author has granted a non-exclusive license allowing Library and Archives Canada to reproduce, publish, archive, preserve, conserve, communicate to the public by telecommunication or on the Internet, loan, distribute and sell theses worldwide, for commercial or non-commercial purposes, in microform, paper, electronic and/or any other formats.

The author retains copyright ownership and moral rights in this thesis. Neither the thesis nor substantial extracts from it may be printed or otherwise reproduced without the author's permission.

AVIS:

L'auteur a accordé une licence non exclusive permettant à la Bibliothèque et Archives Canada de reproduire, publier, archiver, sauvegarder, conserver, transmettre au public par télécommunication ou par l'Internet, prêter, distribuer et vendre des thèses partout dans le monde, à des fins commerciales ou autres, sur support microforme, papier, électronique et/ou autres formats.

L'auteur conserve la propriété du droit d'auteur et des droits moraux qui protègent cette thèse. Ni la thèse ni des extraits substantiels de celle-ci ne doivent être imprimés ou autrement reproduits sans son autorisation.

In compliance with the Canadian Privacy Act some supporting forms may have been removed from this thesis.

Conformément à la loi canadienne sur la protection de la vie privée, quelques formulaires secondaires ont été enlevés de cette thèse.

While these forms may be included in the document page count, their removal does not represent any loss of content from the thesis.

Bien que ces formulaires aient inclus dans la pagination, il n'y aura aucun contenu manquant.


Canada

ABSTRACT

WEI MIN CHENG

M. Sc.

Bioresource Engineering

Microwave Power Control Strategies on the Drying Process

The current study was conducted for evaluating the effects of two different strategies viz., phase control and cycle control, on the microwave/air drying process. A phase-controlled electrical power regulator was developed and connected in series with the original cycle-controlled power regulator of an existing domestic microwave oven. The microwave oven was further modified such that combined microwave and convectional drying can be accommodated.

The system performance was evaluated. It was observed that phase-controlled power regulator could be successfully used for quasi-continuous (fast-switching) power regulation with the maximization of power efficiency. The degradation of output microwave power was recorded and the nonuniform distribution of microwave field in the cavity was also verified.

The effects of phase control and cycle control were evaluated through combined microwave and convective drying of potato samples. Results showed that different power control methods had different impacts on drying kinetics and product quality. In both drying modes, the drying time increased with the decrease of microwave power density and the increase of air velocity. The drying rates of cycle-controlled drying are significantly higher than those of phase-controlled drying. In terms of rehydration capacity the phase-controlled drying mode produced better results. The product colour and sensory attributes were independent of the power control methods.

RÉSUMÉ

WEI MIN CHENG

M. Sc.

Génie des Bioressources

Stratégies de contrôle de l'énergie micro-onde lors du séchage

La présente étude a été entreprise pour évaluer deux stratégies de contrôle d'un processus de séchage micro-onde/air, dont un contrôle du cycle et un contrôle de la phase. Un régulateur de puissance électrique avec réglage de phase a été développé et branché en série avec le régulateur de puissance de base à réglage par cycle existant sur un micro-onde ordinaire. Le micro-onde fut modifié davantage en y combinant un système de ventilation permettant le séchage par convection. La performance du système a été évaluée. Le régulateur avec réglage de phase s'est montré apte à contrôler la puissance de façon presque continue (commutation rapide), avec une optimisation du rendement énergétique. La dégradation de la puissance de sortie a été enregistrée et la distribution non uniforme du champ micro-onde dans l'enceinte a été constatée.

Les effets du contrôle par réglage de phase et du contrôle du cycle ont été évalués par le séchage micro-onde/convectif d'échantillons de pommes de terre. Les résultats ont montré que les différentes méthodes de contrôle de la puissance ont eu un impact différent sur la cinétique du séchage et la qualité des produits. Pour les deux modes de séchage, le temps de séchage a augmenté avec une diminution de l'intensité de puissance micro-onde et l'augmentation de la vitesse de l'air. Les taux de séchage du procédé contrôlé par réglage du cycle sont sensiblement supérieurs à ceux d'un procédé contrôlé par réglage de phase. La capacité de réhydratation a été supérieure lors du séchage contrôlé par réglage de phase. La couleur et les caractéristiques organoleptiques n'ont pas été influencées par la méthode de contrôle de la puissance micro-onde.

ACKNOWLEDGEMENTS

I would like to express my deep gratitude and thanks to my thesis supervisors Drs. G. S. V. Raghavan and M. Ngadi for their guidance, encouragement, and advice throughout the course of my studies, their valuable suggestions for the experimental arrangements, and their patience during the correction of the manuscript.

I am particularly indebted to Dr. T. Ji, Microwave Plasma Lab., College of Physics Electronics, University of Electronics Science & Technology, China, for his advice and support in evaluation of microwave cavity and whole system.

I am very grateful to Professors G. Sun and W. Li, Department of Electronic Information Science and Technology, Nankai University, China, for their guidance and help in design and fabrication of the new triac power regulator, and the counsel in the area of control of power supply to magnetron.

Special thanks to Dr. N. Wang, Dr. S. Sotocinal, Mr. J. Dai, Mr. A. Kulamarva, Ms. A. Tasneem for their contributions and assistance during the preliminary studies on the triac power regulator. I would like to thank Mr. Y. Garipey, Dr. V. Orsat, Mr. V. Changrue, Dr. S. Venkatesh, Mr. Y. Li, and Mr. T. J. Rennie for their help and assistance in various phases during my studies. Thanks to all staff and students of the Department of Bioresource Engineering.

I express my sincere gratitude to all my colleagues from Grand Dryer Co. (Ltd), China, and Nanjing Research and Design Institute for Comprehensive Utilization of Wild Plants, China, for their friendship and encouragement.

Finally, I would like to express my thanks to my wife, Tong, and my daughter, Annie, for their patience, love, and understanding during my studies.

TABLE OF CONTENTS

ABSTRACT.....	ii
RÉSUMÉ.....	iii
ACKNOWLEDGEMENTS.....	iv
TABLE OF CONTENTS.....	v
LIST OF FIGURES.....	viii
LIST OF TABLES.....	xi
LIST OF SYMBOLS.....	xii
CHAPTER I. INTRODUCTION.....	1
1.1 Background.....	1
1.2 Objectives.....	3
1.3 Scope.....	4
CHAPTER II. REVIEW OF LITERATURE.....	5
2.1 Electrical Power Conversion and Control.....	5
2.1.1 Introduction of Power Electronics.....	5
2.1.2 Methods of Power Conversion and Control.....	6
2.1.3 Semiconductor Power Switches.....	6
2.1.3.1 Power Diode.....	7
2.1.3.2 Thyristor.....	8
2.1.3.3 Power Transistor.....	9
2.1.3.4 Comparison of Semiconductor Power Switches.....	9
2.2 Microwaves.....	9
2.2.1 Introduction.....	9
2.2.2 Theory of Microwave Fields.....	12
2.2.2.1 Maxwell's Equations.....	12
2.2.2.2 Plane Waves.....	14
2.2.3 Magnetron.....	15
2.3 Conversion and Control of Electrical Power Supply to Magnetron.....	15
2.3.1 Linear Resistive Control.....	16
2.3.2 Integral Cycle Control.....	17
2.3.3 Pulse Width Modulation.....	18

2.3.4 Phase Control.....	20
2.3.5 Control System for Power Regulator.....	23
2.4 Microwave Drying.....	24
2.4.1 Theory of Microwave Drying.....	25
2.4.1.1 Drying Mechanism.....	25
2.4.1.2 Dielectric Properties.....	25
2.4.1.3 Dielectric Heating Equation.....	26
2.4.1.4 Penetration Depth.....	27
2.4.2 Microwave Drying Equipment.....	27
2.4.3 Microwave Drying Applications.....	28
2.4.3.1 Microwave Convection Drying.....	28
2.4.3.2 Microwave Vacuum Drying.....	30
2.4.3.3 Microwave Freeze Drying.....	31
2.4.3.4 Other Microwave Hybrid Drying.....	32
CHAPTER III. MATERIAL AND METHODS.....	33
3.1 Microwave Drying System.....	33
3.2 Development of Microwave Drying Setup.....	33
3.3 Design of A Triac Phase-controlled Power Regulator.....	35
3.3.1 Triac Phase Controller used in Preliminary Studies.....	35
3.3.2 Design of New Triac Phase-controlled Power Regulator.....	36
3.3.2.1 Selection of Triac Thyristor.....	36
3.3.2.2 Selection of Trigger Unit (Diac).....	37
3.3.2.3 Selection of Timing Unit (RC Oscillator).....	39
3.3.2.4 Design of Snubber Circuit.....	40
3.3.2.5 Design of Heat Sink.....	42
3.3.2.6 Hysteresis Free Unit.....	44
3.3.2.7 RFI Filter.....	44
3.3.2.8 Control System for Power Regulator.....	44
3.3.2.9 Summary.....	45
3.4 Modification of Original Electrical Circuit.....	46
3.5 Instrumentation, Measurements and Control.....	48
3.6 Calorimetric Test.....	49
3.7 Drying Process.....	49
3.8 Quality Evaluation.....	51
3.8.1 Rehydration Capacity.....	51
3.8.2 Colour Analysis.....	52
3.8.3 Sensory Evaluation.....	52
3.9 Statistical Analysis.....	52

CHAPTER IV. RESULTS AND DISCUSSION.....	53
4.1 System Performance.....	53
4.1.1 Calibration of Maximum Microwave Output Power.....	53
4.1.2 Determination of Distribution of Microwave Field Inside Cavity.....	54
4.1.3 Preliminary Studies on a Commercial Triac Phase Controller.....	57
4.1.4 Evaluation of New Triac Phase-controlled Power Regulator.....	59
4.1.4.1 Physical Description of Phase Control Process.....	59
4.1.4.2 Performance of New Triac Phase Controller.....	61
4.2 Drying Modes.....	63
4.3 Drying Characteristics.....	63
4.3.1 Phase-controlled MWA Drying.....	63
4.3.2 Cycle-controlled MWA Drying.....	66
4.3.3 Phase-controlled MWA Drying versus Cycle-controlled MWA Drying.....	66
4.3.3.1 Drying Rate.....	66
4.3.3.2 Material Internal Temperature.....	71
4.4 Quality Evaluation.....	73
4.4.1 Rehydration Capacity.....	73
4.4.2 Colour Analysis.....	74
4.4.3 Sensory Evaluation.....	74
 CHAPTER V. SUMMARY, CONCLUSIONS AND RECOMMENDATIONS.....	 77
5.1 Summary and Conclusions.....	77
5.2 Recommendations.....	79
 REFERENCES.....	 80

LIST OF FIGURES

Figure 2.1	Microwave frequency band in the electromagnetic spectrum.....	11
Figure 2.2	Plane electromagnetic wave showing electric field normal to magnetic field.....	14
Figure 2.3	Magnetron (a) cross section, (b) resonant cavity.....	16
Figure 2.4	Linear resistive control: input and output voltage waveforms.....	17
Figure 2.5	Integral cycle control (a) diagram, (b) input and output voltage waveforms.....	18
Figure 2.6	Pulse width modulation: input and output voltage waveforms.....	19
Figure 2.7	Block diagram of damped resonant inverter circuit.....	19
Figure 2.8	Principle of phase control showing delay angle and conduction angle.....	20
Figure 2.9	Phase control with inductive load (a) simplified diagram, (b) input and output voltage waveforms.....	21
Figure 2.10	Block diagram of a SCR power regulator with close-loop control.....	23
Figure 3.1	Schematics of the microwave drying apparatus showing cavity, air heating and blowing system, sensors, sample holder, and data acquisition system.....	34
Figure 3.2	Photograph of the microwave drying setup showing cavity, air heating and blowing system, display panels, triac power regulator, filament transformer, strain gauge, and data acquisition system.....	35
Figure 3.3	A commercial phase control circuit composed of triac, diac, resistors, potentiometer, diodes, and capacitor.....	36
Figure 3.4	A simplified triac phase control circuit showing three basic components: triac, diac, and RC oscillator.....	37
Figure 3.5	Snubber circuit composed of a resistor and a capacitor.....	41

Figure 3.6	Power dissipation vs. on-state current.....	43
Figure 3.7	Block diagram of proposed triac power regulator.....	45
Figure 3.8	Photograph of the proposed triac power regulator.....	46
Figure 3.9	Block diagrams of (a) original circuit, (b) modified circuit.....	47
Figure 3.10	Photograph of the modified electrical circuit showing proposed triac phase controller and filament transformer.....	48
Figure 4.1	Top view of microwave cavity showing (a) measurement locations, (b) microwave power distribution at different locations.....	55
Figure 4.2	Microwave output power versus applied voltage to HV transformer for preliminary study on a phase controller.....	58
Figure 4.3	Patterns of voltage waveforms (a) input source voltage, (b) voltage applied to HV transformer with the omitting of transient voltage.....	60
Figure 4.4	Microwave output power versus applied voltage to HV transformer for evaluation of new phase controller.....	62
Figure 4.5	Dimensionless moisture content during phase-controlled MWA drying, air temperature at 25°C and air velocity at 0.5m/s.....	64
Figure 4.6	Dimensionless moisture content during phase-controlled MWA drying, air temperature at 25°C and air velocity at 1.5m/s.....	64
Figure 4.7	Dimensionless moisture content during cycle-controlled MWA drying, air temperature at 25°C and air velocity at 0.5m/s.....	67
Figure 4.8	Dimensionless moisture content during cycle-controlled MWA drying, air temperature at 25°C and air velocity at 1.5m/s.....	67
Figure 4.9	Drying rate during drying with power density of 0.994W/g, air temperature at 25°C and air velocity at 0.5m/s.....	68
Figure 4.10	Drying rate during drying with power density of 1.988W/g, air temperature at 25°C and air velocity at 0.5m/s.....	68

Figure 4.11	Drying rate during drying with power density of 0.994W/g, air temperature at 25°C and air velocity at 1.5m/s.....	69
Figure 4.12	Drying rate during drying with power density of 1.988W/g, air temperature at 25°C and air velocity at 1.5m/s.....	69
Figure 4.13	Material temperature during drying with power density of 0.994W/g, air temperature at 25°C and air velocity at 0.5m/s.....	72
Figure 4.14	Material temperature during drying with power density of 1.988W/g, air temperature at 25°C and air velocity at 0.5m/s.....	72

LIST OF TABLES

Table 2.1	Characteristics of semiconductor switches.....	10
Table 2.2	Effects of moisture and frequency on attenuation.....	27
Table 3.1	Principal parameters of triac Q2025R5.....	39
Table 3.2	Principal parameters of diac HT-35.....	40
Table 3.3	Operational parameter during microwave/air (MWA) drying.....	51
Table 4.1	Constant drying rate during two given drying modes.....	70
Table 4.2	Rehydration capacity of dried potato sample.....	73
Table 4.3	Colour parameters of dried potato sample.....	75
Table 4.4	Sensory evaluation of dried potato sample.....	76

LIST OF SYMBOLS

AC	alternative current
a^*	colour coordinate (dimensionless)
BJT	bipolar junction transistor
BWT	back wave tube
b^*	colour coordinate (dimensionless)
\vec{B}	magnetic flux density (weber/m ²)
C_p	heat capacity (cal /g /°C)
CPU	central processing unit
C_s	capacitance of capacitor in snubber circuit (F)
CUJT	complementary unijunction transistor
D	diameter (mm)
DC	direct current
di/dt	maximum rate-of-change of on-state current (A/ μ s)
dv/dt	critical rate-of-rise of off-state voltage (V/ μ s)
$dv/dt(c)$	critical rate-of-rise of commutation voltage (V/ μ s)
$(dv/dt)_{max}$	maximum rate of change of voltage (V/s)
\vec{D}	electric flux density (coulomb/m ²)
EMC	electromagnetic compatibility
E_{rms}	rms electric field (V/m)
E_x	components of electric field (V/m)
E_y	components of electric field (V/m)
E_z	components of electric field (V/m)
\vec{E}	electric field (V/m)
GTO	gate turn-off thyristor

H	height (mm)
H_x	components of magnetic field (ampere/m)
H_y	components of magnetic field (ampere/m)
H_z	components of magnetic field (ampere/m)
\vec{H}	magnetic field (ampere/m)
HV	high voltage
I_{BO}	peak break over current at break over voltage (μA)
I_{CEO}	maximum allowable dc collector current (A)
I_{DM}	drain current (A)
I_{DRM}	peak off-state current (mA)
$I_{F(AV)}$	maximum allowable full cycle average forward current (A)
$I_{F(RMS)}$	maximum allowable full cycle rms forward current (A)
I_{FSM}	maximum allowable nonrepetitive surge current (A)
IGBT	insulated gate bipolar transistor
I_{GT}	DC gate trigger current in specific operating quadrants (mA)
I_{GTM}	peak gate trigger current (mA)
I_H	holding DC current (mA)
I/O	input and output interfaces
I_{rms}	rms load current (A)
ISM	industrial, scientific and medical
I_{TRM}	peak pulse current (A)
$I_{T(RMS)}$	rms on-state current (A)
I_{TSM}	peak one-cycle surge (A)
I^2t	rms surge (non-repetitive) on-state current (A^2/t)
\vec{j}	current density (ampere/m ²)
K	conversion factor (J/cal)
K_1	conversion factor (m ³ /s/W)

L	length (mm)
L_{in}	load inductance (H)
L^*	colour coordinate (dimensionless)
MC_{dl}	dimensionless moisture content
MCT	metal oxide semiconductor controlled thyristor
MOSFET	metal oxide semiconductor field effect transistor
MW	microwave
MWA	microwave/air
N_{off}	cycles in which power is in OFF state
N_{on}	cycles in which power is in ON state
P	MW power density (W/g)
PA	percentage of absorbed microwave power (%)
P_{ab}	absorbed microwave power by water (W)
$P_{ab,i}$	absorbed microwave power by sample i (W)
P_{av}	average power dissipated (W)
P_{avg}	average load power (W)
$P_{D(AV)}$	average power loss generated in junction area (W)
$P_{G(AV)}$	average gate power dissipation (W)
P_{GM}	peak gate power dissipation (W)
PID	proportional, integrating, and differentiating
PL	power level (%)
P_{loss}	average power loss (W)
P_{max}	maximum power (W)
PUT	programmable unijunction transistor
Q_{air}	air flow rate (m^3/s)
R	load resistance (Ω)
RAM	random access memory

RC	resistor & capacitor
R_{cs}	thermal resistance between case and heatsink ($^{\circ}\text{C} / \text{W}$)
RFI	radio frequency interference
R_{jc}	thermal resistance between triac junction and case ($^{\circ}\text{C} / \text{W}$)
ROM	read only memory
R_s	resistance of resistor in snubber circuit (Ω)
R_{sa}	thermal resistance between heatsink and surrounding ambient air ($^{\circ}\text{C} / \text{W}$)
SBS	silicon bilateral switch
SITH	static induction thyristor
rms	root mean square
SCR	silicon controlled rectifier
t	heating time (s)
T_{air}	modulated air temperature ($^{\circ}\text{C}$)
T_{amb}	ambient temperature ($^{\circ}\text{C}$)
$\tan\delta$	loss tangent (dimensionless)
t_{gt}	gate controlled turn-on time (μs)
T_{jpeak}	peak junction temperature ($^{\circ}\text{C}$)
UJT	unijunction transistor
V	volume of dielectric material (m^3)
V_A	air velocity (m/s)
V_{BO}	break over voltage (V)
V_{CEO}	maximum allowable collector-emitter voltage (V)
V_{DRM}	repetitive peak blocking voltage (V)
V_{DSS}	drain source voltage (V)
V_{GT}	DC gate trigger voltage (V)
V_{max}	peak supply voltage (V)

V_{rms}	rms load voltage (V)
V_{RRM}	maximum allowable reverse repetitive voltage (V)
V_S	peak transient voltage (V)
V_{TM}	peak on-state voltage at maximum rated rms current (V)
W	width (mm)
WG	water gain (%)
W_s	sample weight (g)
W_{st}	sample weight at time t during rehydration (g)
W_{s0}	sample weight at time zero during rehydration (g)
X	sample moisture content (kg/kg, dry basis)
x_f	sample final moisture content (% , wet basis)
X_f	sample final moisture content (kg/kg, dry basis)
x_i	sample initial moisture content (% , wet basis)
X_i	sample initial moisture content (kg/kg, dry basis)
$ Z $	impedance (Ω)
α	trigger delay angle (rad)
β	conduction angle (rad)
Δ	angle (rad)
ΔT	temperature rise ($^{\circ}C$)
ΔV_{BO}	break over voltage symmetry (V)
$ \Delta V_{\pm} $	dynamic break back voltage (V)
$\Delta\kappa''/\Delta M$	slope (dimensionless)
ε	permittivity of the medium (farad/m)
e	Napierian logarithmic base
ε_0	permittivity of free space (farad/m)
η	intrinsic impedance (Ω)
κ'	dielectric constant (dimensionless)

κ''	dielectric loss (dimensionless)
κ^*	dielectric permittivity (dimensionless)
μ	permeability of the medium (henry/m)
ρ	charge density (coulomb/m ²)
Σ	summation operator
Φ	sinusoidal angle of the load impedance (rad)
ω	angular frequency (rad/s)
χ	extinction angle (rad)
∂	partial differential coefficient
∇	vector operator

CHAPTER I. INTRODUCTION

1.1 Background

Drying, by definition, involves removal of a liquid from a solid, semi-solid, or liquid material to produce a solid product by supplying thermal energy to cause a phase change, which converts the liquid to vapor (Mujumdar, 2003). Modern drying operations have been used for decades in foodstuff, chemical, pharmaceutical, cosmetic, and agricultural industries. During conventional air drying process heat transfer is limited by the low thermal conductivity of biomaterials, the low energy efficiency, and the prolonged drying time. The moisture evaporating rate is high at the beginning of the air heating but falls rapidly with the reduction of moisture content during the falling rate period. The use of microwaves can eliminate these problems by the fast and effective thermal process.

The application of microwaves is of increasing interest in processing of foods and bio-commodities over past two decades. The main advantages of microwave processing come from its ability of high-energy conversion efficiency, rapid heat transfer process, and volumetric heating. During microwave drying process local pressure and temperature rise continuously even though the loss factor of treated materials decrease with the reduction of moisture content (Zhou et al., 1994; Metaxas and Meredith, 1983). Although these increases of pressure and temperature can speed up the drying process, they may cause side effects such as bio-value degradation, physical damages, and non-uniform temperature distribution in treated materials (Shivhare et al., 1991; Yongsawatdigul and Gunasekaran, 1996).

The fact that the input electrical power or the output microwave power governs the quality of final products has led many researchers to study the relationship between them. Shivhare et al. (1992a) employed intermittent microwave operation in corn drying, the data indicated that seed quality corn could be obtained using 5min on and 15min off pulse at 0.5 W/g absorbed power. Shivhare et al. (1992b) claimed the microwave power

density should be less than 0.25 W/g if seed-grade corn is desired during continuous microwave drying. Prabhanjan et al. (1995) observed a power level of 50% (rated power of 600W) caused burning of the product in microwave drying of carrots. Venkatachalapathy and Raghavan (2000) found that at 40% power duty cycles (rated power of 600W), there was burning of the dried strawberry in microwave drying of whole strawberries. Sunjka (2003) conducted intermittent microwave drying of cranberries and the results illustrated that for obtaining higher quality dried cranberries, pulsed modes with longer power-off time (30s on and 45s off), higher power density and lower system pressure should be applied. Similar studies were also carried out by Raghavan et al. (1993) in microwave drying of cereal grain, Raghavan and Silveira (2001) in microwave drying of strawberries and Sanga et al. (2001) in microwave drying of sensitive materials. These studies optimized microwave drying processes and, as a result, product qualities were improved.

Extensive research studies have been done on the optimization of drying process either by integral cycle control (intermittent or ON/OFF microwave operation) or by linear resistive control (continuous microwave operation) of input electrical power. However, no report emphasized the effects of other input electrical power control methods, such as fast switching method, on the microwave drying process.

Practically, the input electrical power to magnetron can be controlled by following methods:

- Integral cycle control (ON/OFF) by a time-controller – The applied power is always 100% of the rating during ON portions of duty cycles; and 0% of the rating during OFF portions. The operating time is comparatively lengthy. Either ON or OFF time is at least in seconds. The product temperature is pulsated, reaches a maximum during ON and then decreases during OFF portion (Tulasidas, 1994; Sunjka 2003).
- Linear resistive control (continuous) by a variable ratio transformer or a resistor – This method was predominantly used for the regulation of the magnitude of voltage

in the early days of electrical engineering. The output current flows through the controlling resistance and produces a huge power loss. The power consumption is always 100% rated power no matter what power value was actually used. The poor power efficiency is unbearable in practical applications (Trzynadlowski, 1998; Ross, 1997). Nowadays these controllers are only used in situations in which the issue of power efficiency is not of major importance.

- Phase-control (fast switching, or quasi-continuous) by a triac or two SCRs based controller – The input voltage waveform is sliced (switched on) one time at each half wave. The switching frequency is 100 or 120 times per second. Power is controlled by the regulation of the electrical phase angle. The output voltage waveform appears as a distorted sinusoid.
- Pulse width modulation (fast switching, or quasi-continuous) by a power transistor based controller – The input voltage waveform is sliced (switched) more than one time at each half wave. Supply power is switched as high as 2,000 times per second. The output voltage is determined by the pulse width.

Each power control method produced its own unique time-varying supply voltage waveforms (profiles). Different supply voltage waveform may give different effects on the microwave drying process. Hence there is a need to investigate their impacts on drying performances.

1.2 Objectives

The main objective of this study is to evaluate the effects of two different input electrical power control methods, phase control and cycle control, on the microwave/air drying process. The specific objectives to achieve the main goals are:

- To design a phase-controlled electrical power regulator (phase controller).
- To modify an existing domestic microwave oven such that combined microwave and convectional drying could be achieved; and the input electrical power to magnetron

could be cycle controlled, phase controlled, or combined cycle/phase controlled.

- To evaluate the system performance which included calibration of the maximum microwave output power, determination of the microwave distribution in the cavity, establishment of the relations between the output power and the input voltage for the phase-controlled power regulator.
- To conduct drying tests and evaluate the effects of two input power control methods, cycle control and phase control, on the microwave/air drying process and product qualities.

1.3 Scope

The development of new microwave drying unit was based on an existing domestic microwave oven. For the compatibility reason, only two input electrical power control methods were evaluated; the other two methods, linear resistive control and pulse width modulation were excluded out of the study. Furthermore, only single-phase electrical power supply was considered in this study.

CHAPTER II. REVIEW OF LITERATURE

2.1 Electrical Power Conversion and Control

2.1.1 Introduction of Power Electronics

Power electronics, covering the conversion and control of electrical power using semiconductor power switches, has developed from mechanical and magnetic conversion technologies that are more than one hundred years old (Krein, 2001; Mazda, 1993; Heumann, 1985; Pearman, 1980). In the middle of 1800s the mechanical periodical switches came into use as commutators in electrical machines. The first directional switching valves were developed at the beginning of 1900s. In the meantime, uncontrolled rectifiers were developed for the purpose of battery charging. The first semiconductor rectifiers, such as copper oxide rectifiers and selenium rectifiers, were employed in 1930s for rectification purposes in the lower power range. The semiconductor diodes, germanium diodes and silicon diodes, made from monocrystalline semiconductor materials were developed in early 1950s. With the introduction of transistors and the magnetic amplifiers in 1950s, power conversion and control techniques were greatly improved.

The modern version of power electronics began in the latter part of the 1950s when the first silicon-controlled rectifier thyristor (SCR), a kind of semiconductor power switches, was made in 1957 in the laboratories of the General Electric Company in the USA. This marked the beginning of power conversion and control from mechanical and magnetic devices to electric devices. In the course of further development of the power switches included bi-directional gate-controlled thyristor (triac) in 1960s; integrated circuit (IC), gate turnoff thyristor (GTO) and metal-oxide semiconductor field effect transistor (power MOSFET) in 1970s; insulated-gate bipolar transistor (IGBT) in 1980s, and nowadays the metal-oxide semiconductor controlled thyristor (MCT).

2.1.2 Methods of Power Conversion and Control

Power conversion and control include AC-DC, DC-DC, DC-AC and AC-AC conversions (Fisher, 1991; Datta, 1985).

AC-DC conversions, also called AC-DC rectifications, convert AC power to the DC power. AC-DC conversions include uncontrolled and controlled rectifications. The uncontrolled rectifications are rectified by power diodes. In controlled rectifications the AC line voltage source are usually converted by thyristor phase-controlled rectifiers to a unidirectional source and filtered to approximate DC power.

In DC-DC power conversion, a DC voltage of one value is converted to another DC voltage, either larger or smaller. DC-DC conversion is also named DC-DC chopping. Traditional DC-DC conversions use the control resistors to perform the operations. Nowadays semiconductor power switches such as thyristors are used which eliminate the energy consumption in the control resistors.

DC-AC conversion, also called DC-AC inversion, converts the DC source voltage to the alternating voltage. The output AC voltage is not a sinusoid but a rectangular or stepped waveform.

AC-AC conversions include AC-AC voltage control with fixed frequency, AC-AC frequency conversion with variable voltage, AC-DC-AC conversion, etc. In AC-AC voltage control, a variable AC voltage is obtained from an AC voltage input. Integral cycle control and phase control are two basic configurations for this method. In AC-AC frequency conversion, an AC output of variable frequency with variable voltage is synthesized by cycloconverters. The output frequency is a fraction of input frequency. In AC-DC-AC conversion, AC power is rectified first to produce an intermediate DC stage which is then inverted to produce a variable AC output.

2.1.3 Semiconductor Power Switches

Power conversion and control are obtained with the application of power

regulators. The main components in the power regulators are the power switches. Two types of power switches, electromechanical switches and semiconductor switches, are available for power control purposes. Compared to their electromechanical counterparts, semiconductor power switches have the advantages of fast response and reliable performance. The representative semiconductor power switches include the power diodes, the thyristors, and the power transistors (Mazda, 1993; Rashid, 1988; Heumann, 1985). These switches are constructed from monocrystalline semiconductor material. The base materials are exclusively silicon monocrystals. The ideal semiconductor power switches should have the following characteristics (Trzynadlowski, 1998):

- High ratings of voltage and current, to allow high power level operation with a single switch.
- Low leakage current and voltage drop across the switch in the off state, to minimize power losses.
- Short turn on and off transitions, to allow high frequency switching with minimum losses.
- Low power requirements to switch on and off, to simplify the control circuits and improve the efficiency and reliability of the whole converter.
- Negative temperature coefficient on the conducted current, to result in equal current sharing by paralleled devices.
- High ratings of dv/dt and di/dt , to limit the use of auxiliaries for protection of the switch from failures and structural damages.
- Low price, to enhance the competence.
- Large safe operating areas, both the forward bias and reverse bias ones.

2.1.3.1 Power Diode

The power diode is a pn junction element for conducting current that has little forward voltage drop and small reverse current flow. The differences between power

diode and ordinary diode are in that power diode has larger power, current and voltage handling capacities. The power diodes are rated for reverse voltage and forward current. The reverse voltage rating is the maximum allowable reverse repetitive voltage, V_{RRM} . Several ratings for the forward current are the maximum allowable full cycle average forward current, $I_{F(AV)}$, the maximum allowable full cycle rms forward current, $I_{F(RMS)}$, and the maximum allowable nonrepetitive surge current, I_{FSM} . For safe operation none of the above ratings should be exceeded.

2.1.3.2 Thyristor

The thyristor is a multi-layer pn junction element for conducting current. The prominent elements in this family are silicon controlled rectifier thyristor (SCR), bi-directional gate controlled thyristor (triac), gate turn-off thyristor (GTO), metal oxide semiconductor controlled thyristor (MCT), static induction thyristor (SITH), and bi-directional diode thyristor (diac). In SCR, triac, and GTO the main current flows only after an input gate current flows through the device. The SCR conducts only unidirectional current and blocks the reverse current, while the triac can conduct bi-directional currents. The GTO is similar in construction to a SCR, but it can be turned off by a negative gate current. The MCT is similar in operation to the GTO, but it is turned on and off by gate voltage not gate current. The diac is a five-layer device without a gate, which is used to trigger other semiconductor power switches.

The important parameters of the thyristor are the rms on-state current conduction angle of 360° , $I_{T(RMS)}$; repetitive peak blocking voltage, V_{DRM} ; peak off-state current, I_{DRM} ; peak on-state voltage at maximum rated rms current, V_{TM} ; peak gate trigger current, I_{GTM} ; peak one-cycle surge, I_{TSM} ; critical rate-of-rise of off-state voltage at rated V_{DRM} , dv/dt ; and maximum rate-of-change of on-state current, di/dt . Above ratings are the ones that a thyristor can withstand without harmful effects.

2.1.3.3 Power Transistor

The power transistors include the bipolar junction transistor (BJT), metal oxide semiconductor field effect transistor (power MOSFET), and insulated gate bipolar transistor (IGBT). A power BJT does not differ significantly from that of an ordinary transistor, except that the capacities of power, voltage and current are greater. The power MOSFET is used for replacing the power BJT in the situations where high switching frequencies are needed. The IGBT combines the advantages of BJT and power MOSFET with lower conduction losses and higher voltage and current ratings.

The rated current of a BJT represents the maximum allowable DC collector current, I_{CEO} . The rated voltage of BJT is the maximum allowable collector-emitter voltage that the transistor can safely block with a zero base current, V_{CEO} . For the power MOSFET the rated voltage is the drain source voltage, V_{DSS} , and the rated current is the drain current, I_{DM} .

2.1.3.4 Comparison of Semiconductor Power Switches

The characteristic comparisons of semiconductor power switches are listed in Table 2.1.

2.2 Microwaves

2.2.1 Introduction

Microwaves are the electromagnetic waves that radiate from electrical disturbances at higher operation frequencies between 300MHz and 300GHz, the corresponding wavelengths range from 1m to 1mm. The microwave frequency band in the electromagnetic spectrum is illustrated in Figure 2.1. In electronics domain, when operation frequency is relatively low, the storage, flow, and the potential difference of the electric charges are the main targets for study; while the electromagnetic fields generated by the electric charges are neglected. But at higher operating frequency the effects of

electromagnetic fields become dominant. The electromagnetic radiation is the main issue in the study of microwaves.

Table 2.1 Characteristics of semiconductor switches (Source: Trzynadlowski, 1998)

Type of Switch	Control Signal	Control Characteristic	Switching Frequency	On-state Voltage Drop	Maximum Voltage Rating	Maximum Current Rating
Diode				medium	6.5kV	5kA
SCR	current	trigger ¹	low	medium	4kV (6kV ^a)	3kA (4kA ^a)
Triac	current	trigger ¹	low	medium	1kV	50A
GTO	current	trigger	low	medium	6.5kV	4kA
BJT	current	linear	medium	low	1.5kV	1kA
MOSFET	voltage	linear	very high	high	1kV	150A
IGBT	voltage	linear	high	medium	1.5kV	1kA

Superscript a: Light activated thyristors.

Electromagnetic waves first came into use in the middle of 1800s with the development of electric telegraph and optics (Carter, 1990). Microwaves were originally developed as a new field of electromagnetic waves during World War II for the use of navigation and radar target detection. Since then this field has been developing at a fast pace. Nowadays microwaves are widely used in many areas (Scott, 1993; Gardiol, 1984):

- Communication such as satellite communication, radio and TV broadcasting, wireless cable systems – The high frequency and very large bandwidths indicate microwaves are suitable for communication links. Microwave communications are easily coupled with satellite because they can pass through the ionosphere which

reflects low frequency radio signals.

- Radar such as detection, navigation, traffic control, searching, radio measurement and microwave radiometry – Microwaves penetrate fog and clouds, travel straight and give distinct shadows and reflections so that they can be used for distance and direction measurement and in radar systems.
- Industrial, scientific, medical (ISM) applications such as microwave heating and drying, microwave measurement, linear acceleration, plasma containment and radio astronomy – Microwaves are absorbed by water so that they can be used for heating and drying. Many atoms and molecules resonate at microwave frequency and are adequate for scientific measurement. The allowed ISM frequencies are 915; 2,450; 5,800; and 22,125 MHz which are surrounded by frequency bands for communication and radar purposes.

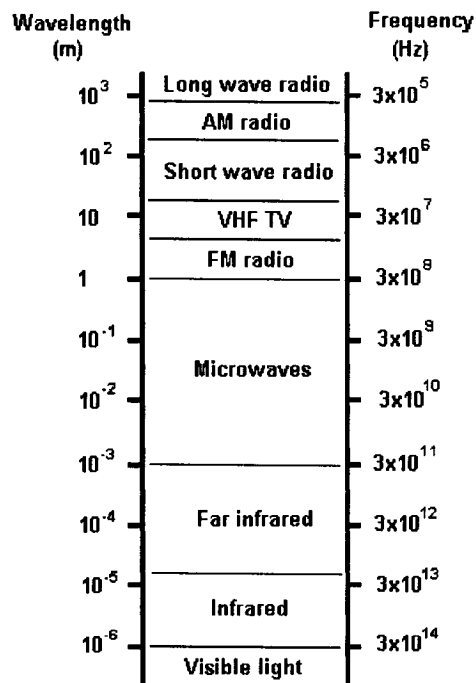


Figure 2.1 Microwave frequency band in the electromagnetic spectrum

2.2.2 Theory of Microwave Fields

2.2.2.1 Maxwell's Equations

Microwave fields are the electromagnetic fields at specific operational frequencies. Electromagnetic fields are comprised of electric fields and magnetic fields which are dependent on each other. The fundamental time-varying governing equations for electromagnetic fields, called Maxwell's laws which were a combination of four basic laws, were established in 1873 by James Clerk Maxwell. The four equations include (Fuller, 1990):

$$\nabla \cdot \vec{D} = \rho \quad (2.1)$$

$$\nabla \cdot \vec{B} = 0 \quad (2.2)$$

$$\nabla \times \vec{E} = -\frac{\partial \vec{B}}{\partial t} \quad (2.3)$$

$$\nabla \times \vec{H} = \vec{J} + \frac{\partial \vec{D}}{\partial t} \quad (2.4)$$

where:

∇ = vector operator

\vec{D} = electric flux density (coulomb/m²)

\vec{B} = magnetic flux density (weber/m²)

\vec{E} = electric field (V/m)

\vec{H} = magnetic field (ampere/m)

\vec{J} = current density (ampere/m²)

ρ = charge density (coulomb/m²)

∂ = partial differential coefficient

The first law is called Gauss' theorem of electrostatics; which describes the flux of the electric flux density vector out of a closed surface equal to the total free charges

enclosed. The second law is Gauss' theorem of magnetostatics; which states that the flux of the magnetic flux density out of a closed surface is zero. The third law is called Ampere's law; which explains the line integral of the magnetic field around a closed path is equal to the total current flux through a surface bounded by that path. The fourth law is Faraday's law of electromagnetic induction; which illustrates the line integral of the electric field around a closed path is equal to the rate of change of the magnetic flux through a surface bounded by that path. Maxwell's laws describe the facts that the electric fields are produced by still electric charges and/or time-dependent magnetic fields; and the magnetic fields are generated by moving electric charges and/or time-variant electric fields. The relations between the electric flux density, \vec{D} ; the magnetic flux density, \vec{B} ; the electric field, \vec{E} ; the magnetic field, \vec{H} ; and the current density, \vec{J} are given by the properties of the medium in which microwaves exist:

$$\vec{B} = \mu\vec{H} \quad (2.5)$$

$$\vec{D} = \epsilon\vec{E} \quad (2.6)$$

$$\vec{J} = \sigma\vec{E} \quad (2.7)$$

where:

μ = permeability of the medium (henry/m)

ϵ = permittivity of the medium (farad/m)

The microwaves are usually sinusoidal. The general solutions to Maxwell's equations for the sinusoidal waveforms in a non-conducting medium with no initial stored charges are:

$$\nabla^2\vec{E} + \omega^2\mu\epsilon\vec{E} = 0 \quad (2.8)$$

$$\nabla^2\vec{H} + \omega^2\mu\epsilon\vec{H} = 0 \quad (2.9)$$

where:

ω = angular frequency (rad/s)

2.2.2.2 Plane Waves

The simplest solution of Maxwell's equations is the plane wave solution. The properties of plane wave include (Fuller, 1990): (1) no fields act in the z-direction of propagation; (2) an electric field normal to the magnetic field; (3) no variation of field in the plane perpendicular to the z-direction of propagation; (4) both fields act in a direction along the plane of the wave; (5) the electric and magnetic fields are in phase with each other. The electric and magnetic field in a plane electromagnetic wave are shown in Figure 2.2. The properties of a plane wave propagating in the z-direction can be specified by following equations,

$$E_x = \eta H_y \quad E_y = -\eta H_x \quad E_z = H_z = 0 \quad (2.10)$$

and,

$$\eta = \sqrt{\frac{\mu}{\epsilon}} \quad (2.11)$$

where:

E_x, E_y, E_z = components of electric field (V/m)

H_x, H_y, H_z = components of magnetic field (ampere/m)

η = intrinsic impedance (Ω)

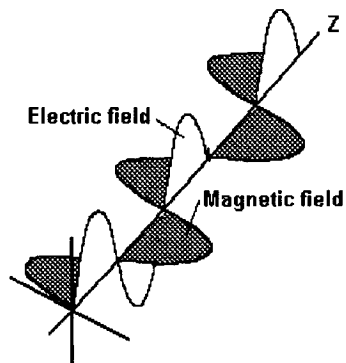


Figure 2.2 Plane electromagnetic wave showing electric field normal to magnetic field

2.2.3 Magnetron

Microwave can be generated by either thermionic devices such as magnetron, klystron, back wave tube (BWT), and gyrotron; or solid-state devices such as microwave transistors and diodes. Among these generators the magnetron is most widely used for the industrial applications.

Figure 2.3 illustrates the structure of magnetron which takes a coaxial structure. The main components of the magnetron include filament, inside cylindrical cathode, outside tubular anode, magnet, exit passage, antenna, vane, and strip ring (Gallawa, 1999; Van Zante, 1973). The electrons are emitted from the cathode which is heated by the internal filament. If there is no magnet the electrons will be accelerated and directed to the anode. With the presence of the magnet the combined electric and magnetic fields will bend the trajectory of the electrons. The static magnetic field is along the axis and the static electric field is radial. The electrons reach the anode through the whirling movements. The anode is constructed with a number of resonator cavities. As the electrons come close to the anode, they pass by the resonator cavities which causes the electrons to oscillate at a very high frequency, usually in a microwave oven, at 2,450MHz. The high-frequency oscillations of the electrons are picked up by an antenna which is located at the output of the magnetron. The microwave fields emitted from the antenna are transmitted through the wave-guide and to the cavity.

2.3 Conversion and Control of Electrical Power Supply to Magnetron

Several methods have been used to control the output microwave power in the microwave applicators. They are: (1) control of the supplied electric power to magnetron (Gallawa, 1999; Meredith, 1998), (2) control of the magnetic field strength inside magnetron (Meredith, 1998; Ishii, 1990), and (3) control of microwave electromagnetic fields inside applicator (Bows, 2001; Bows, 1997; Fritz, 1988; Metaxas and Meredith, 1983).

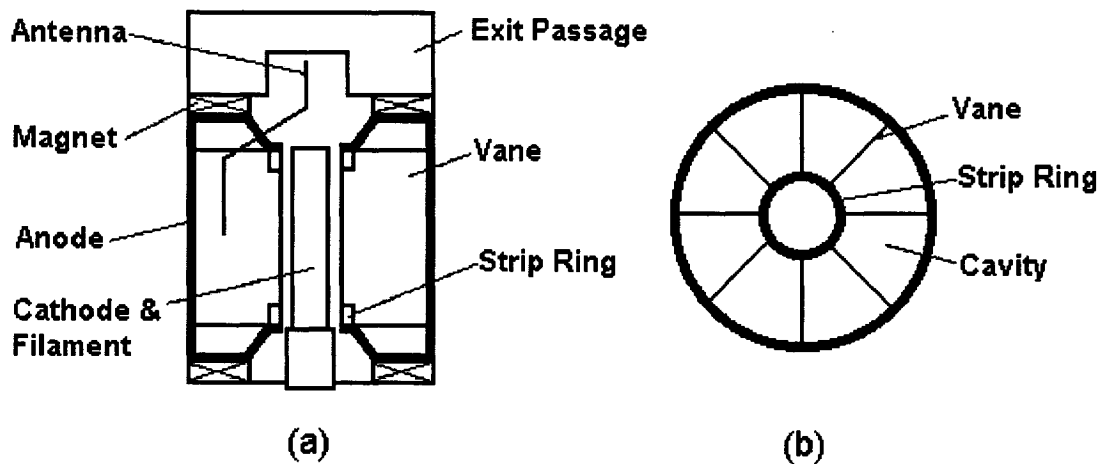


Figure 2.3 Magnetron (a) cross section, (b) resonant cavity

Electrical power delivered to the magnetron can be regulated by varying the value of input AC voltage. Techniques developed for adjusting the single-phase input voltage for microwave equipment include (Meredith, 1998; Neas and Collins, 1988): linear resistive control (continuous), integral cycle control (intermittent or ON/OFF), pulse width modulation (fast switching or quasi-continuous), and phase control (fast switching or quasi-continuous). Power conversion and control are realized by power regulator. The main components in the power regulator are power switches (Datta, 1985; Pearman, 1980).

2.3.1 Linear Resistive Control

In a linear resistive regulator the load voltage and current are adjusted through a resistive device. The load current flows through the controlling resistor which converts excessive electric energy to heat. The power consumption is always in full power level no matter what power level is actually used. Typical linear regulators include variac, potentiometer, rheostat, etc. The main advantages of linear resistive control are: (1) the magnitude of voltage can be adjusted continuously and simultaneously, and (2) the output waveform is exactly the same as input waveform except the magnitude is changed (Figure

2.4).

Linear resistive control is predominantly used in the early days for continuous regulation of voltage level for various industrial applications. Because of significant power dissipation nowadays it is only used where the power level is low and the energy efficiency is not of a main concern (Trzynadlowski, 1998).

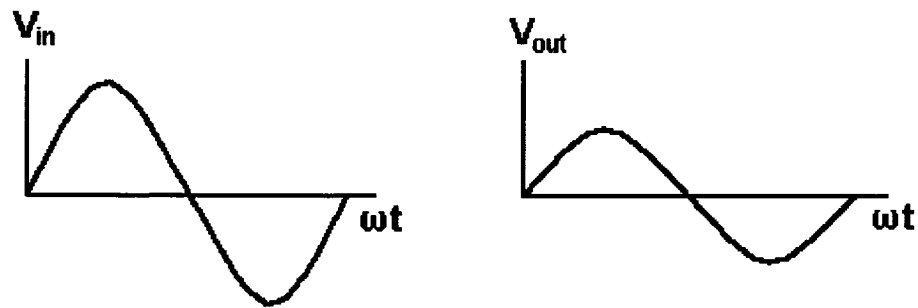


Figure 2.4 Linear resistive control: input and output voltage waveforms

2.3.2 Integral Cycle Control

Integral cycle control is the most widely used method to control the power in domestic and commercial microwave equipments. This method is effected by changing the number of full cycles applied (ON cycles) compared to the number of cycles when the supply is not connected to the load at all (OFF cycles). The relation of ON cycles to OFF cycles is arranged such that the average load voltage and power is achieved. The components of the regulator include a timer and a thyristor power switch. Figure 2.5(a) shows the diagram of an integral cycle control circuit in a microwave oven with a triac thyristor power switch. Figure 2.5(b) shows the profiles of input and output voltage.

The operating time period is relatively long and at least in seconds. Load voltage and load power being controlled from 0 to 100% of the related maximum values. The load power can be calculated from the number of applied cycles during each period:

$$P_{avg} = P_{max} \left(\frac{N_{on}}{N_{on} + N_{off}} \right) \quad (2.12)$$

$$PL = \frac{P_{avg}}{P_{max}} \times 100\% \quad (2.13)$$

where:

PL = power level (%)

P_{avg} = average load power (W)

P_{max} = maximum power (W)

N_{on} = cycles in which power is in ON state

N_{off} = cycles in which power is in OFF state

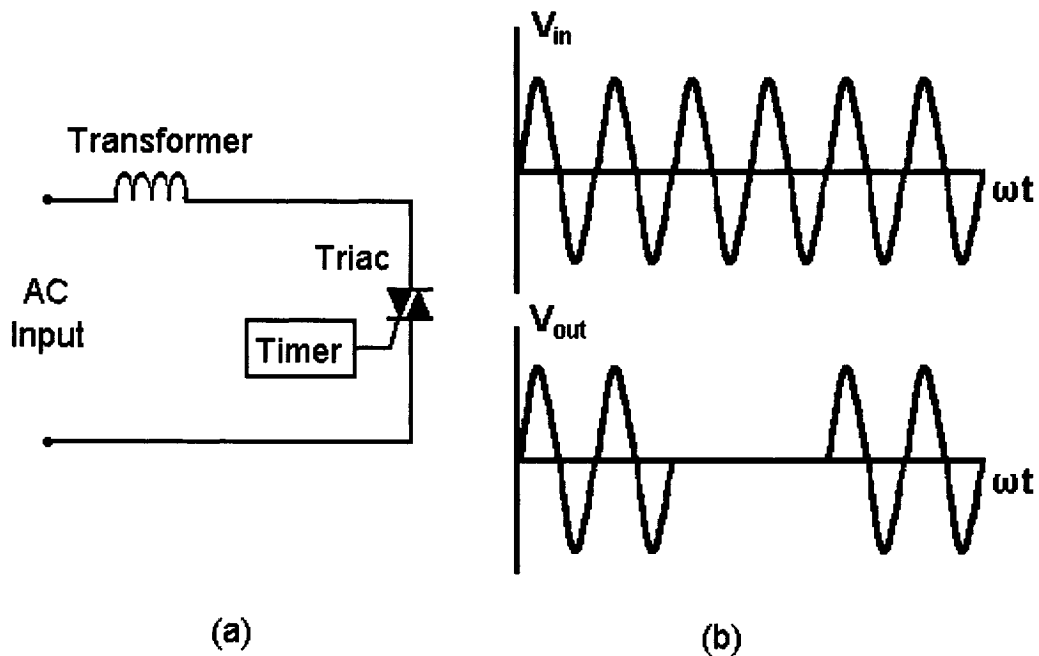


Figure 2.5 Integral cycle control (a) diagram, (b) input and output voltage waveforms

2.3.3 Pulse Width Modulation

Pulse width modulation is a relatively new technique for power regulation in the

domestic and commercial microwave oven. The power switch is switched on and off as high as 20 times during a half cycle of the input voltage. The output voltage is determined by the pulse width. Switching operation is carried out by the power transistors such as IGBT (insulated-gate bipolar transistor). Figure 2.6 shows the profiles of input and output voltage waveforms. Pulse width modulation circuit may take different configurations. Figure 2.7 shows one of them, called damped resonant inverter circuit, which is employed in microwave equipment (Chambers and Scapellati, 1994).

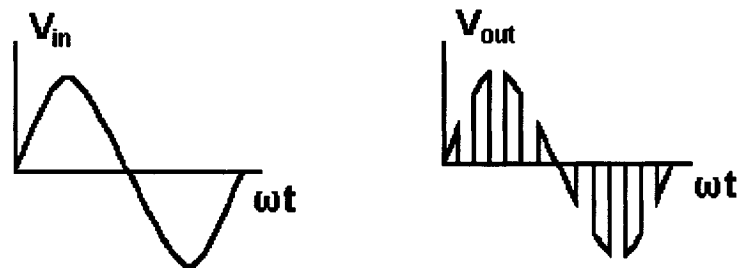


Figure 2.6 Pulse width modulation: input and output voltage waveforms

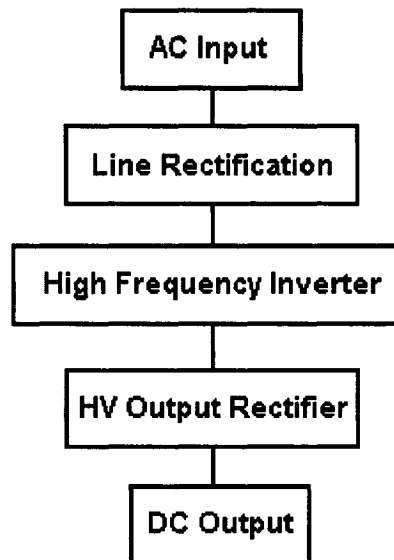


Figure 2.7 Block diagram of damped resonant inverter circuit

2.3.4 Phase Control

Unlike the pulse width modulation technique in which the power switch is turned on and off up to 20 times during a half cycle, the phase control method only allows one time switching during each half-cycle. For the 60Hz AC power input, the number of switching is 120 times per second. The load voltage and power are controlled with the applications of thyristors. The triac thyristors are commonly used for lower current rating while the SCR thyristors for higher current rating. Phase control is achieved by varying the electrical phase angle of the applied AC voltage waveform (Fisher, 1991; Finney, 1980). Figure 2.8 shows the principles of phase control. The delay angle, α , is the number of electrical degrees of the applied AC voltage waveform during which the thyristor is in OFF state, that is, the main current is blocked by the thyristor. The conduction angle, β , is the number of electrical degrees of the applied AC voltage waveform during which the thyristor is in ON state, that is, the main current flows through the load. The relationship between the two angles is $\alpha + \beta = \pi$.

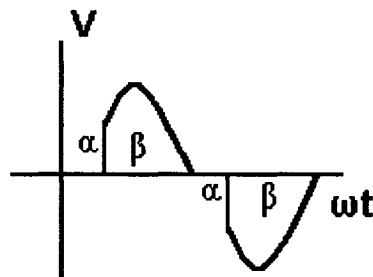


Figure 2.8 Principle of phase control showing delay angle and conduction angle

In actual applications most loads have inductance, such as motors, solenoids, and transformers. The high voltage transformer in the microwave equipment is an inductive load. Figure 2.9(a) shows the principles of an AC voltage phase-controller with a transformer load. Figure 2.9(b) shows the general pattern of voltage waveforms.

Because of the load inductance, the SCRs or triac continue conducting for a

limited angle until reach the extinction angle, χ (Figure 2.9). If the extinction angle, χ is equal or larger than trigger delay angle, α , full output waveform is obtained. If it is less than delay angle the load voltage will be discontinuous. For a resistive load the extinction angle is zero. The rms value of the load voltage, the rms value of the load current, and the average value of power can be calculated by the following equations (Shepherd et al., 1995):

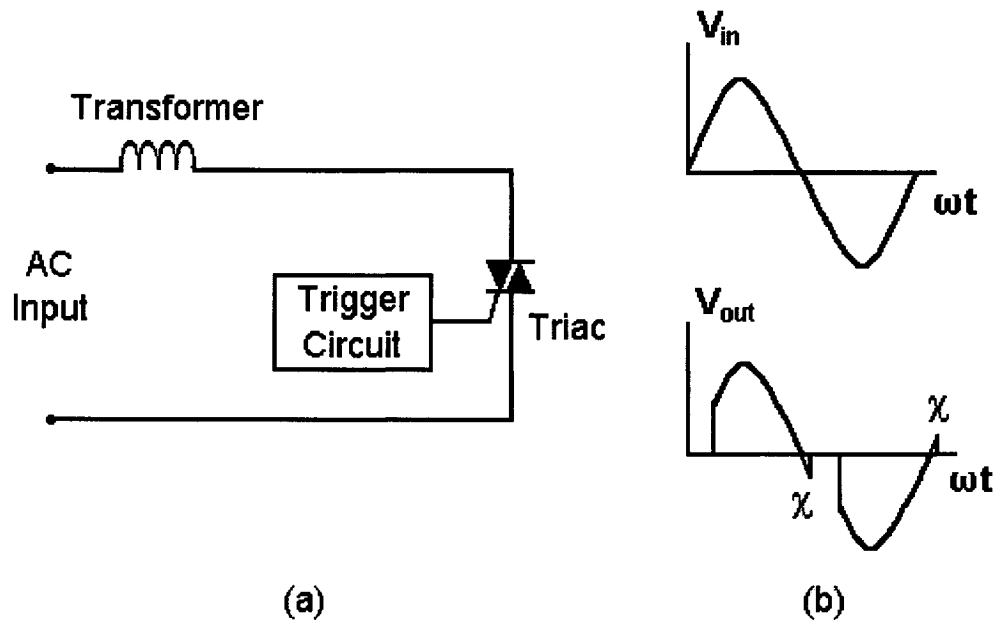


Figure 2.9 Phase control with inductive load (a) simplified diagram, (b) input and output voltage waveforms

$$V_{\text{rms}} = \frac{V_{\text{max}}}{\sqrt{2\pi}} \left(\chi - \alpha + \frac{\sin 2\alpha}{2} - \frac{\sin 2\chi}{2} \right)^{\frac{1}{2}} \quad (2.14)$$

$$I_{\text{rms}} = \frac{V_{\text{max}}}{|Z|\sqrt{2\pi}} \left[\begin{aligned} & \left(\chi - \alpha \right) - \frac{1}{2} \left[\sin 2(\chi - \Phi) - \sin 2(\alpha - \Phi) \right] \\ & + \frac{\sin^2(\alpha - \Phi)}{\cot \Phi} \left[1 - \varepsilon^{2\cot \Phi(\alpha - \Phi)} \right] \\ & + 4 \sin \Phi \sin(\alpha - \Phi) \left[\sin \chi \varepsilon^{\cot \Phi(\alpha - \chi)} - \sin \alpha \right] \end{aligned} \right]^{\frac{1}{2}} \quad (2.15)$$

$$P_{\text{avg}} = \frac{V_{\text{max}}^2}{|Z|4\pi} \left[\frac{\sin(2\alpha - \Phi) - \sin(2\chi - \Phi) + \cos\Phi(2\chi - 2\alpha)}{+ 4\sin\Phi\sin(\alpha - \Phi)} \left[\sin(\Phi + \chi)\varepsilon^{\cot\Phi(\alpha - \chi)} - \sin(\Phi + \alpha) \right] \right] \quad (2.16)$$

and,

$$\chi = \pi + \Phi - \Delta \quad (2.17)$$

$$|Z| = \sqrt{R^2 + L_{\text{in}}^2 \omega^2} \quad (2.18)$$

$$\Phi = \tan^{-1} \frac{\omega L_{\text{in}}}{R} \quad (2.19)$$

where:

I_{rms} = rms load current (A)

L_{in} = load inductance (H)

P_{avg} = average load power (W)

R = load resistance (Ω)

V_{rms} = rms load voltage (V)

V_{max} = peak supply voltage (V)

$|Z|$ = impedance (Ω)

α = trigger delay angle (rad)

ε = Napierian logarithmic base

Δ = angle (rad), $0 \sim 0.01389$ (rad) for small phase angles and $0.02778 \sim 0.06944$ (rad) for large phase angle

χ = extinction angle (rad)

ω = angular frequency (rad/s)

Φ = sinusoidal angle of the load impedance (rad)

Metaxas and Meredith (1983) described a phase-controlled power regulator with close-loop feedback used in the microwave equipment (Figure 2.10). The supply power was automatically regulated by the feedback signal which was the anode current of magnetron. Two SCR thyristors were used to control the AC power supply to the high voltage transformer. The thyristors were turned on by a trigger unit. The trigger unit was

directed by an electronic processor which included comparators, amplifiers and filter. This system was claimed being capable of good long-term stability.

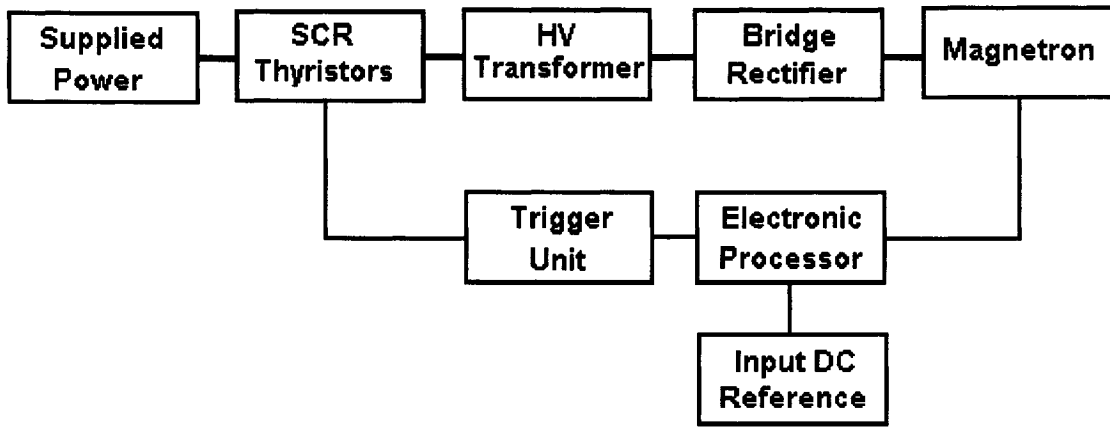


Figure 2.10 Block diagram of a SCR power regulator with close-loop control

2.3.5 Control System for Power Regulator

The control system for a power regulator can take the forms of open-loop control or close-loop control. In open-loop there is no feedback of the output. In the case of a close-loop the controlled variables are continuously detected and adjusted to the desired values. The controlled variables for the microwave processing could be the magnetron anode current (Meredith, 1998), and the temperature of treated materials (Prothon et al., 2001; Kok et al., 1994; Ramaswamy et al, 1991). In modern on-line automatic control system the microprocessors, microcontrollers, fuzzy logic controller, neurocontroller and other digital signal processors are introduced for control of power switches (Trzynadlowski, 1998; Jumah et al., 1995; Laster, 1981). A microprocessor is comprised of the central processing unit (CPU), random access memory (RAM), read only memory (ROM), and input and output interfaces (I/O). A microcontroller is actually a microprocessor specially designed for digital control purposes.

2.4 Microwave Drying

The theory and equipment of microwave drying were developed with the appearance of microwave generator in 1940s. The pioneer elaborated work conducted by Von Hippel to obtain the material properties in the frequency between 100 to 10^{10} Hz established a solid basis for the industrial applications of microwaves (Metaxas and Meredith, 1983). The first commercial scale microwave equipment, a conveyORIZED system, was induced in 1960s in Cryodry Corporation, USA (Decareau, 1985). Currently microwaves have already had their positions in many industrial applications including drying, heating, tempering, sintering, vulcanization, pasteurization, sterilization, blanching, rendering and cooking. These microwave processing systems all operated at 915 MHz and 2,450 MHz. The many advantages of microwave drying technique are summarized below (Sanga et al., 2000; Venkatachalapathy, 1998; Roussy and Pearce, 1995):

- Instantaneous start-up and rapid heating increases production, reduces product cost and labor.
- Higher inside temperature than outside gives rise to a pressure gradient which drives the vapor to the surface.
- Selecting heating and drying due to the greater dielectric losses of water as compared to the product to be dried.
- Volumetric distributions of energy within the material improve quality and avoid surface limitations.
- Thorough drying of wet materials with low thermal conductivity.
- Economy of energy can be realized because of rapid heating and the inherent property of non-heating of the environment.
- Electromagnetic heating is non-polluting, easy to apply and to be automated.

2.4.1 Theory of Microwave Drying

2.4.1.1 Drying Mechanism

When a dielectric material, a poor conductor, is exposed to microwave fields, dielectric heating occurs. Two physical concepts, dipole oscillation of polar molecules and ionic movements, make contribution to the dielectric heating. The polar molecules are randomly oriented in the materials if there is no microwave field exists. With the presence of the alternating microwave fields the molecules tend to align the electric field vector by oscillating at high frequencies of 2,450 MHz. High frequency oscillations produce friction which lead to instantaneous heat generation. The ions dissolved in the materials respond to an alternating microwave fields by repeated acceleration. Huge amounts of collisions happen between the accelerated ions which translate kinetic energy into heat. Microwave heating and drying are also dependent on the physical states of the polar molecules and ions. For the bound molecules and associated ions their responses to microwave fields are hindered compared to the free molecules and ions. For drying process the most common polar molecules are the water molecules. The ionic movement mechanism is less important than the molecule oscillation in the drying process.

2.4.1.2 Dielectric Properties

Besides reflection and transmission of microwave energy, dielectric material has ability to absorb and dissipate considerable amounts of energy in electromagnetic fields. The energy dissipation results in heat generation. These phenomena are due to the material's dielectric property called dielectric permittivity. The dielectric permittivity, κ^* , include dielectric constant, κ' , and dielectric loss, κ'' , which has following relationship (Decareau and Peterson, 1986; Copson, 1975):

$$\kappa^* = \kappa' - j\kappa'' \quad \tan \delta = \frac{\kappa''}{\kappa'} \quad (2.20)$$

where:

$\tan \delta$ = loss tangent (dimensionless)

κ^* = dielectric permittivity (dimensionless)

κ' = dielectric constant (dimensionless)

κ'' = dielectric loss (dimensionless)

During microwave drying process the dielectric permittivity and dielectric loss are variable because of the decreasing of the moisture content. For the free water the dielectric loss decreases rapidly with the diminishing of moisture while in bound water state the slope ($\Delta\kappa''/\Delta M$) is relatively small. These indicate the dipole rotations of bound water molecules are deterred by the surroundings such that the changes of dielectric loss become less and less. The temperature also has strong influence on the dielectric loss in the course of drying operation. In a general way, the dielectric loss decreases with increasing temperature when the temperature is above freezing point.

2.4.1.3 Dielectric Heating Equation

For the biological materials the interactions between materials and magnetic fields can be negligible because of the lower magnetic permeability. The generated heat is considered as the interactions of dielectrics and the electric fields. The relations between dissipated power, the loss factor, the electric field, and the frequency can be derived from Maxwell's laws (Metaxas and Meredith, 1983). With the assumptions of plane waveform of microwaves, constant electric field, and no interactions with magnetic fields, the dielectric heating equation is given by:

$$P_{av} = \omega \varepsilon_0 \kappa'' E_{rms}^2 V \quad (2.21)$$

where:

P_{av} = average power dissipated (W)

ε_0 = permittivity of free space (farad/m)

E_{rms} = rms electric field (V/m)

V = volume of dielectric material (m^3)

The dielectric heating equation demonstrates that the power is proportional to the

loss factor and frequency and selection of the highest of electric field will maximize the power absorption. Because of the restriction of breakdown voltage the electric field is not unlimited.

2.4.1.4 Penetration Depth

The penetration depth is defined as the distance from the surface of material at which the microwave power falls to 37% of its original value, that is, 63% of power is absorbed by the material (Decareau, 1985). At frequencies of 915 MHz and 2,450 MHz, when other parameters are constant, the penetration depths are about two and one half times higher at 915 MHz than those at 2,450MHz. Table 2.2 illustrates the effects of moisture and frequency on attenuation depth.

Table 2.2 Effects of moisture and frequency on attenuation (Source: Decareau, 1985)

Moisture	Dielectric constant, κ'	Loss tangent, κ''/κ'	Penetration depth (cm)	
			915 MHz	2,450 MHz
High	60	0.25	8.4	3.1
Medium	20	0.20	11.7	4.4
Low	10	0.15	22.1	8.2

2.4.2 Microwave Drying Equipment

Microwave drying uses wave-guide to deliver microwave power from the generator to applicator in which microwave is applied to the product. Microwave applicators can be (1) the resonant cavity systems, which are either batch type or continuous type, and (2) wave-guide systems, which are usually continuous type. The resonant cavity systems are actually a microwave oven with any possible size. The continuous resonant cavity applicators can be a single long cavity or multiple small

cavities in series with a conveyor belt passing through the cavities. The wave-guide systems are typically constructed of wave-guides into which the workload is carried by a conveyor and exposed to microwaves. The majority of energy is coupled with the workload and the rest is absorbed by a terminated load. This kind of applicators can be operated empty without damaging the power source. The standard wave-guide systems are only suitable for the moderate and high loss materials. For low loss materials special devices called resonant wave-guide applicators are built.

Besides using the single microwave drying technique, the microwave dryer can be built such that combined drying of microwave with vacuum or convection can be accommodated. More details about microwave equipments can be found in many publications (Kudra and Mujumdar, 2002; Sanga, 2002; Bessarabov et al., 1999; St-Denis, 1998; Schiffmann, 1995).

2.4.3 Microwave Drying Applications

Microwave drying has been shown to be very effective but also costly. Because of this reason, many methods have been proposed to reduce the effective cost of microwave drying. The combined microwave dryings are considered to be the best way to achieve this purpose. Common combination techniques include microwave-convection, microwave-vacuum, microwave-freezing, and microwave-heat pump drying, etc (Kudra and Mujumdar, 2002; Sanga, 2002).

2.4.3.1 Microwave Convection Drying

Shivhare et al. (1991) studied the combination drying of corn with a surface wave applicator. Increasing the absorbed power level increased the drying rate and outgoing air temperature, and considerably reduced the total drying time. Heat loss carried by the outgoing air was minimized by using variable power operation. Germination and bulk density of seed corn was affected by both magnitude and period of microwave power

level.

The drying kinetics and quality of combined microwave and convective drying of grapes in a single mode cavity was studied by Tulasidas et al. (1995). The effects of power density, air temperature and velocity on drying kinetics were analyzed. Higher microwave power density and air temperature resulted in higher drying rates. Increase of air velocity decreased material temperature such that the drying time was increased. It was also observed that microwave dried raisins were lighter in colour than hot air dried samples. Darkness and damage in raisins were dependent on power density, air temperature, and air velocity. Increase in air velocity resulted in better quality raisins whereas the microwave power and air temperature had the opposite effect.

Ren and Chen (1998) carried out a series of experiments to determine drying characteristics of American ginseng roots in a microwave-hot air environment in a modified experimental microwave oven. The microwave power was controlled by a microprocessor from 10 to 1000 W at 10W increments. Drying was conducted until the desired moisture content was achieved. Results illustrated that the combined drying method was very efficient for drying American ginseng roots with the drying time reduced by 28.7 to 55.2%, and had little influence on the colour of the final product.

Jumah and Raghavan (2001) used the combined microwave-convective batch spouted bed drying technique to dry wheat to analyze heat and mass transfer phenomena. The governing equations were established with the consideration of internal heat generation and thermal diffusion. Results showed combined drying gave a higher drying rate than in convectional method alone. Increasing microwave electric field strength, frequency, and inlet air temperature raised the sample temperature, increased drying rates and reduced drying time. Air velocity did not influence the drying rate noticeably but did affect material temperature.

Simultaneous application of microwave power and hot air to dehydrate apple cylinders in order to analyze the drying kinetics was conducted by Andres et al. (2004).

The microwave power was set at 0, 3, 5, 7, and 10W/g combined with air at 25, 30, 40 and 50°C. Air velocity was 1m/s in all tests. The drying kinetics was analyzed by the continuous weighing of the sample weight. Results showed that the drying kinetics was affected by the microwave power, the air temperature and the pretreatments. The tissue characteristics observed illustrated that the process variables not only affected the drying kinetics but also altered the macro and microstructure of the final product.

2.4.3.2 Microwave Vacuum Drying

Some materials are damaged or decompose at high temperatures, so it is preferable if drying takes place at the reduced boiling points (Jones and Rowley, 1996). Compared to conventional vacuum drying, heat transfer rate in microwave-vacuum drying is increased greatly and the final product uniformity is excellent. Drouzas and Schubert (1996) investigated the process of microwave vacuum drying of banana slices. They concluded that this type of drying is preferable to conventional drying in order to avoid product degradation due to high temperatures encountered in convective drying. The microwave vacuum drying produced final product of excellent quality as examined by taste, aroma, smell and rehydration tests.

Lin et al. (1998) used carrot slices to conduct vacuum microwave dryings to compare air drying and freeze drying on the basis of rehydration, color, density, nutritional value, and textural properties. Vacuum microwave dried carrot slices had higher rehydration capacity, higher α -carotene and vitamin C content, lower density, and softer texture than those prepared by air drying. Although freeze drying yielded a product with improved rehydration, appearance, and nutrient retention; the vacuum microwave drying was rated equal or better than freeze drying in terms of color, texture and flavor.

Drouzas et al. (1999) used a laboratory microwave/vacuum drier for drying kinetic experiments with fruit gels. The system was operated in the vacuum range of 30-50 mbar and microwave power range of 640-710W. Results indicated that the drying rate constant

of the thin-layer model of drying of fruit gel was found to increase with increasing microwave power and decreasing absolute pressure. The color of the microwave-vacuum dried fruit gel was significantly lighter than the color of the microwave-air dried product.

A comparative study of microwave/convective and microwave/vacuum drying of cranberries was carried out by Sunjka (2003). The cranberry fruits were mechanically and osmotically pretreated before subjecting it to drying. Quality parameters were color, textural properties, and organoleptic properties. Drying process with different power densities and power ON/OFF duration cycling was evaluated. The energy efficiency of the process was emphasized. Results showed that microwave/vacuum drying had a promising overall potential for high-quality products compared to microwave/convective drying. The color values were similar; the organoleptic properties exhibited slight preference to microwave/convective drying. For the textural properties, microwave/vacuum had better results. The results also illustrated microwave/vacuum drying to be more energy-efficient than microwave/convective drying.

2.4.3.3 Microwave Freeze Drying

Freeze drying involves the sublimation of ice to water vapor without passing through the liquid phase. A comparison of conventional (CD) freeze drying and microwave (MW) freeze drying of frozen peas was performed by Cohen et al. (1992). Drying time, rehydration ratio, shear press of texture, color and sensory rating were evaluated. The MW freeze drying decreased the drying time significantly. The peas with MW freeze drying had a greater rehydration ratio than those with CD freeze drying. For the color and sensory properties there was no significant difference between the two types of freeze drying.

Litvin et al. (1998) conducted dehydration experiments, in which the carrots could be dried by freeze drying (FD); by a combination of freeze, microwave, and air drying (FMA); or by a combination of freeze, microwave, and vacuum drying (FMV). In FMA

and FMV processes, the carrots were first freeze dried to a moisture of 40%, then treated by microwaves for 50s and finally dried to 5% moisture in forced air or vacuum. In FD the carrots were freeze-dried to the final product moisture content. The color, dimensions, and rehydration ratio of FMA dried products were similar to those of FD dried products. FMV had some beneficial effect on color. Fast drying was achieved by FMA compared to FD.

2.4.3.4 Other Microwave Hybrid Drying

Jia (1992) developed a prototype dryer with a heat pump of 5kW and a microwave power of 10kW. The purpose was to investigate the performance and feasibility of heat pump assisted microwave drying. A mathematical model was developed to predict the steady state performance of a heat pump assisted continuous microwave drying process. A three dimensional finite element algorithm was developed to predict the microwave distributions in the material. Drying tests using foam rubber and vegetables were conducted. The experimental results indicated that the heat pump assisted microwave drying was comparable to convective drying in energy consumption while with a much higher drying speed.

A study of the combination of infrared, microwave, and convective drying of cellular concrete was carried out in an experimental kiln by Glouannec et al. (2002). The results showed that using infrareds in the early drying stage increased in surface temperature and sped up evaporation. This advantage lasted until the surface was dried up. Similarly, energy generated in the core of material induced by microwave boosted the water transfer from the core to the surface. As a result, the combination of infrared, microwave, and convective drying allowed rapid, homogeneous and efficient operation.

CHAPTER III. MATERIAL AND METHODS

3.1 Microwave Drying System

Microwave drying system was developed based on a commercial microwave oven (Magnasonic MMMW5730, LG Electronic Inc., Korea) with nominal power of 700W at 2,450 MHz. Dimensions of cavity are 300×195×290mm (L×H×W) with the volume of 0.117m³. The original control set-up (power regulator) in the microwave oven included a power switch and a timer. The power regulator worked based on the integral cycle control method, that is, power level is either 100% or 0% of rated values. The developmental work included,

- Development of microwave drying setup,
- Design of a triac phased-controlled power regulator (phase controller),
- Modification of original electrical circuit.

3.2 Development of Microwave Drying Setup

An air heating and blowing system was introduced for the purpose of coupling microwave with air drying. As the first step, the turnable was dismantled and removed from the cavity. A circular opening with a diameter of 150mm was then made at the bottom of the oven. Through the opening the microwave cavity was connected to an air heater and an axial air fan via a plastic duct. Two electrical heating coils with a total rated power of 2kW were located inside the duct between the axial fan and the cavity. An axial air fan with nominal power of 0.25kW was placed near the air inlet of the pipe. A metallic screen filter was fixed to the air inlet. To prevent leakage of microwave energy from the applicator, a perforated metallic plate was fitted to the circular opening. The diameter of each perforation was 5mm. The extra function of the perforated plate was to have uniform air distribution.

A small hole was drilled on the top of microwave cavity through which the sample

holder was connected to a strain gauge (load cell) located on the top of the oven. The sample holder comprised of a Teflon frame with an attached fine mesh resin screen at the bottom. The sample holder designed was strong and heavy enough so that the stream of the air flow would not disturb the measurement of the sample weight. Inside cavity a Teflon guide pipe of $\Phi 150 \times 100 \text{ mm}$ (D \times H) was fitted to the opening such that the air stream was directed to the base of sample holder. A microwave leakage detector (DJF-2000, Nankai, China) was used to insure there was no leakage through the openings and the perforations. As far as the requirement of the vapor outlet is concerned, the original outlet provided was adequate for the new setup to exhaust the vapor; no further modification work was done about the vapor outlet. Figure 3.1 shows schematics of the microwave drying setup. Figure 3.2 illustrates photograph of the whole microwave drying system, the electrical aspects of the system will be introduced next.

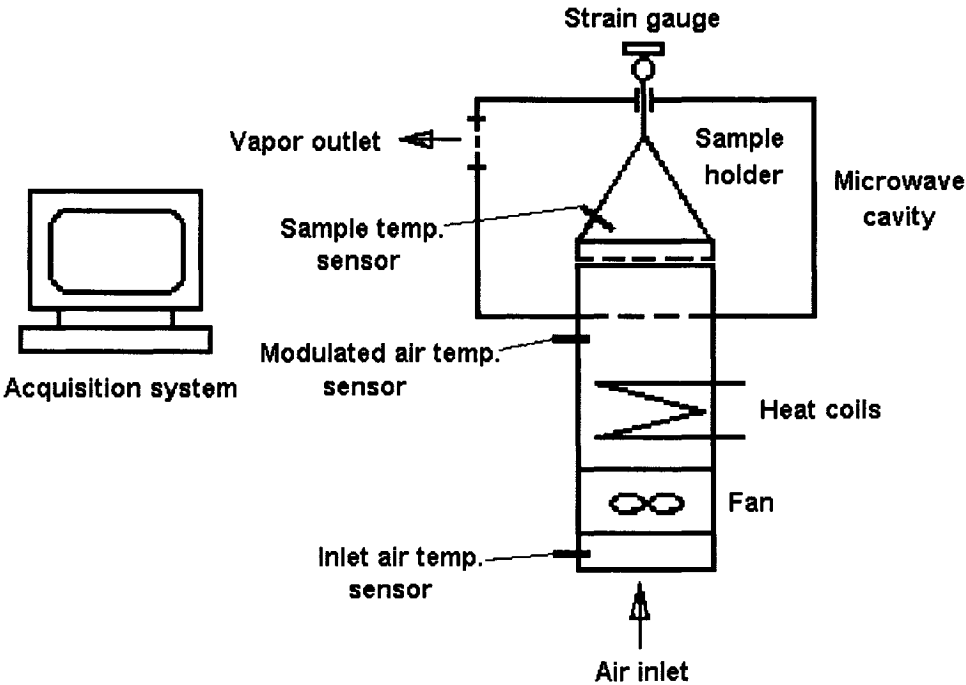


Figure 3.1 Schematics of the microwave drying apparatus showing cavity, air heating and blowing system, sensors, sample holder, and data acquisition system



Figure 3.2 Photograph of the microwave drying setup showing cavity, air heating and blowing system, display panels, triac power regulator, filament transformer, strain gauge, and data acquisition system

3.3 Design of a Triac Phase-controlled Power Regulator

In this study a new phase-controlled power regulator was designed for the phase control purpose. The phase-controlled power regulator (phase controller) was connected in series with the existing integral cycle-controlled power regulator (cycle controller) such that supplied power can be either cycle-controlled or phase-controlled.

3.3.1 Triac Phase Controller used in Preliminary Studies

A commercial circuit (Figure 3.3) originated from the Company of Teccor Electronics, USA was used as a basic circuit for preliminary studies. This circuit was initially designed for the resistive load such as lamp, heater, etc. The three main parts of the circuit were a power switch which was a triac thyristor, a trigger unit which was a diac

thyristor, and a timing unit which included two resistors (R_1 , R_4) and a capacitor (C_1). The other components were used to enhance the performance of the circuit.

In preliminary studies three circuits, named from #1 to #3, were built based on Figure 3.3. The circuit #1 with the triac current rating of 10A was connected in series to a 40W incandescent lamp. The circuits #2 with the triac current rating of 10A was connected in series to the primary winding of the high voltage (HV) transformer of existing microwave oven. The circuit #3 with the triac current rating of 20A was also connected to the microwave oven as circuit #2.

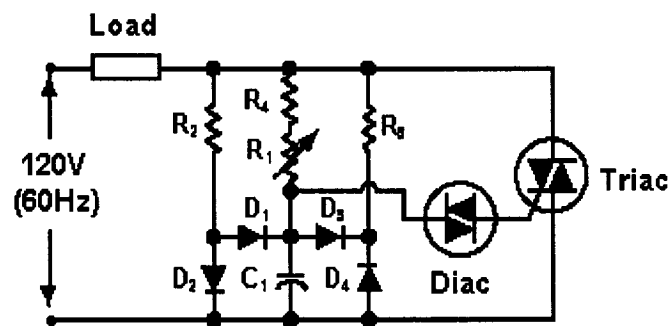


Figure 3.3 A commercial phase control circuit composed of triac, diac, resistors, potentiometer, diodes, and capacitor (Source: Teccor Electronics, 2003)

3.3.2 Design of New Triac Phase-controlled Power Regulator

Because of the inadequacies of the commercial phase controller used in the preliminary studies, a new triac phase-controlled power regulator was developed and used for the current microwave drying studies.

3.3.2.1 Selection of Triac Thyristor

The triac thyristor is a semiconductor power switch and has no moving parts to turn-on or turn-off an electrical circuit. The bistable characteristics, high-energy efficiency, mature technique, and long life expectancy make the triac thyristor very

popular in the AC power conversion and control applications compared to other power switches. In this study a triac thyristor is being used.

The triac is a three-terminal switch with two main terminals and one gate terminal. The two main terminals are connected to the main circuit and the gate terminal is used to switch on and off the triac (Figure 3.4). Shepherd et al. (1995) stated the most important factors for making the optimal choice of power switch are the voltage and current ratings. Laster (1981) concluded that the key to selecting a proper thyristor is the consultation of the manufacturers' specification sheets based on the load characteristics such as voltage, current and power. For the given task, the steady state voltage was 120V and the steady state current 8.2A. The actual triac current rating was taken as three times as steady state load requirement (Ramshaw, 1975) and the voltage rating was the same as the steady state value. Referring to the product data sheets of Teccor Electronics (2003) the triac of the Part Number of Q2025R5 was chosen. The rms (root mean square) on-state current, $I_{T(RMS)}$, is 25A. The repetitive peak block voltage, V_{DRM} , is 200V. Table 3.1 shows principal parameters of triac Q2025R5.

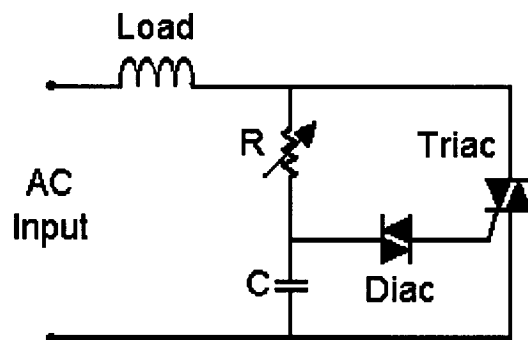


Figure 3.4 A simplified triac phase control circuit showing three basic components: triac, diac, and RC oscillator

3.3.2.2 Selection of Trigger Unit (Diac)

A triac can be triggered (turned on) by many ways, such as thermal triggering,

radiation triggering, voltage triggering, transient voltage triggering and gate current triggering. The gate current triggering is the most commonly used to fire triac. In gate current triggering, a gate current that has sufficient magnitude and duration turns triac into conducting state from off state. Phase control requires the triac to repetitively conduct both positive and negative half-cycles. The trigger signal should be synchronized to supply voltage. The same power source for both triac and its trigger unit is the most commonly used approach in favor of this synchronization. In the proposed controller, gate current triggering and same power source strategies were adopted.

Sun et al. (2000) introduced a developed triggering method for the synchronization purpose. The triac was triggered by the pulses generated by a microprocessor. Since main circuit and microprocessor used separated voltage sources, a zero-crossing circuit was introduced to identify the zero-crossing points of the main voltage and to realize the synchronization.

Trigger units cover the unijunction transistor (UJT), complementary unijunction transistor (CUJT), programmable unijunction transistor (PUT), silicon bilateral switch (SBS), and diac. The diac trigger device was chosen in this design for triggering triac. The diac is another kind of thyristor. The difference between diac and triac is in that diac has two main terminals without gate terminal. One terminal is connected to the timing unit and the other terminal is attached to the gate terminal of triac (Figure 3.4).

The diac is turned on by voltage break over method. At low voltage levels, the reverse-biased junction prevents any current except a small leakage current. When the applied voltage is increased to the break over voltage, V_{BO} , the diac is in conduction; gate current flows through diac to the gate terminal of triac. The gate current increases with the decreasing of the voltage across the diac.

Referring to the product data sheets of Teccor Electronics (2003), the diac with a Part Number HT-35 was chosen with the break over voltage, V_{BO} , of 30 to 40 V. Table 3.2 shows principal parameters of diac HT-35.

Table 3.1 Principal parameters of triac Q2025R5 (Source: Teccor Electronics, 2003)

Parameter	Specific test conditions	Rating
$I_{T(RMS)}$	Rms on-state current with conduction angle of 360°	25A (max)
V_{DRM}	Repetitive peak blocking voltage	200V (min)
I_{GT}	DC gate trigger current in specific operating quadrants; $V_D = 12$ V dc	QI: 50mA (max) QIII: 50mA (max)
I_{GTM}	Peak gate trigger current	100mA
V_{GT}	DC gate trigger voltage; $V_D = 12$ V dc; $R_L = 60$	$T_C = 25^\circ\text{C}$: 2.5V(max)
P_{GM}	Peak gate power dissipation; $I_{GT} \leq I_{GTM}$	20W
$P_{G(AV)}$	Average gate power dissipation	20W
I_{DRM}	Peak off-state current, gate open; $V_{DRM} =$ maximum rated value	$T_C = 25^\circ\text{C}$: 0.1mA(max) $T_C = 100^\circ\text{C}$: 1mA (max) $T_C = 125^\circ\text{C}$: 3mA (max)
V_{TM}	Peak on-state voltage at maximum rated rms current	$T_C = 25^\circ\text{C}$: 1.8V(max)
I_H	Holding DC current; gate open	100mA(max)
I_{TSM}	Peak one-cycle surge	60Hz: 200A 50Hz: 167A
$dv/dt(c)$	Critical rate-of-rise of commutation voltage at rated V_{DRM} and $I_{T(RMS)}$	5V/ μ s
dv/dt	Critical rate-of-rise of off-state voltage at rated V_{DRM} gate open commutating $di/dt = 0.54$ rated $I_{T(RMS)}$ /ms; gate unenergized	$T_C = 100^\circ\text{C}$: 400V/ μ s(min) $T_C = 125^\circ\text{C}$: 275V/ μ s(min)
t_{gt}	Gate controlled turn-on time; $I_{GT} = 200$ mA with 0.1 μ s rise time	4 μ s
I^2t	Rms surge (non-repetitive) on-state current for period of 8.3 ms for fusing	166A ² s
di/dt	Maximum rate-of-change of on-state current; $I_{GT} = 200$ mA with ≤ 0.1 μ s rise time	100 A/ μ s

3.3.2.3 Selection of Timing Unit (RC Oscillator)

Timing unit is to arrange the conduction time of the triac. A RC oscillator, comprised of a capacitor and a potentiometer, was adopted as the timing unit to produce the trigger (gate) current and to control the conduction time of the triac (Figure 3.4). The magnitude and the direction of the gate current were determined by the RC oscillator. The

conduction time was determined by the RC time constant. Different conduction time was obtained by varying the resistance value of the potentiometer. The capacitance and maximum resistance were chosen such that the delay angle can vary from 0° to 180° during each half cycle.

Table 3.2 Principal parameters of diac HT-35 (Source: Teccor Electronics, 2003)

Parameter	Specific test conditions	Rating
V_{BO}	Break over voltage	30V (min), 40V (max)
ΔV_{BO}	Break over voltage symmetry	3V (max)
$ \Delta V_{\pm} $	Dynamic break back voltage	10V (min)
I_{BO}	Peak break over current at break over voltage	25 μ A(max)
I_{TRM}	Peak pulse current for 10 μ s, 120PPS, $T_A \leq 40^\circ\text{C}$	2A(max)

3.3.2.4 Design of Snubber Circuit

The load of the proposed power regulator was the transformer that converted input low voltage to the high voltage to activate the magnetron for generating electromagnetic microwaves. Transformer switching is a regular and significant source of transient overvoltage.

For the transformer load, the turn-off of a triac thyristor might induce a high transient voltage across the triac thyristor. Since the triac is in series with the transformer, it would attempt to turn off at the instant the current passes through zero value. The supply voltage would lead the current in a relatively large phase angle and the rate-of-rise of off-state voltage across the thyristor, dv/dt , begins to overshoot. The value of dv/dt should be below the rating value given in the data sheet of the manufacturer otherwise serious problems would be induced. If the commutating dv/dt of the circuit was larger than the dv/dt capacity of the triac, the triac might be either burned out or returned to on-state without applying any gate signal.

In order to eliminate the side effects of the dv/dt during turn-off period, a snubber

circuit connected across the triac was introduced into the triac voltage controller. Figure 3.5 shows snubber circuit used to reduce turn-off voltage transient. Also, the snubber could reduce the magnitude of surge voltage.

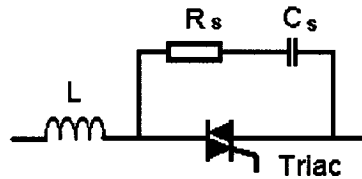


Figure 3.5 Snubber circuit composed of a resistor and a capacitor

The maximum rate of change of voltage, $(dv/dt)_{\max}$, can be calculated by using the following equations (Datta, 1985):

$$(dv/dt)_{\max} = \frac{V_s}{\sqrt{L_{in} C_s}} \quad (3.1)$$

$$R_s = \sqrt{\frac{L_{in}}{C_s}} \quad (3.2)$$

where:

$(dv/dt)_{\max}$ = maximum rate of change of voltage (V/s)

V_s = peak transient voltage (V)

L_{in} = load inductance (H)

C_s = capacitance of capacitor in snubber circuit (F)

R_s = resistance of resistor in snubber circuit (Ω)

From the above equations values of R_s and C_s could be calculated. However, the voltage across the thyristor is determined not only by the L , R_s and C_s but also including other resistors, capacitors and inductors in the network. Also the selection of the values of R_s and C_s depended on the circuit configuration. For the planned snubber circuit the R_s was 100Ω while C_s was $0.1 \mu\text{F}$. For the transformer load, the rate of change of current, di/dt , was not a serious issue, because the inductance of the transformer would suppress

the di/dt.

3.3.2.5 Design of Heat Sink

In the phase control circuit the heat generated in the thyristor due to switching operation must be removed to limit the junction temperature to a reasonable value. An increase in junction temperature can increase turn-on time and reduce breakdown voltage. The critical junction temperature usually lies between 120 to 150°C. Usually a heatsink is used to conduct the heat away from the thin wafer of silicon. The heatsink should have relative large surface to dissipate the heat into ambient air. Due to low weight, high thermal conductivity and good heat storage ability, aluminum is generally used as sink material. The shape of the sink varies from a flat piece to elaborate fins. There are three mechanisms, conduction, convection and radiation through which heat is transferred through the sink to the ambient. Air cooling, especially forced air cooling, is by far the most used and most practical method. Flat piece heatsink and forced air-cooling were adopted in the current design.

The peak junction temperature for the given case happens when trigger delay angle is zero. The peak junction temperature, T_{jpeak} , could be calculated by (Finney, 1980),

$$T_{jpeak} = T_{amb} + P_{loss} (R_{jc} + R_{cs} + R_{sa}) \quad (3.3)$$

where,

T_{jpeak} = peak junction temperature (°C)

T_{amb} = surrounding ambient air temperature (°C)

$P_{D(AV)}$ = average power loss generated in junction area (W)

R_{jc} = thermal resistance between triac junction and case (°C /W)

R_{cs} = thermal resistance between case and heatsink (°C /W)

R_{sa} = thermal resistance between heatsink and surrounding ambient air (°C /W)

For the triac Q2025R5 the average power loss generated in the junction area,

$P_{D(AV)}$, could be found from Figure 3.6, which was 8 Watts. Based on the product data sheets the thermal resistance between triac junction and case was $0.89\text{ }^{\circ}\text{C}/\text{W}$. Assuming $R_{cs} = 1.2\text{ }^{\circ}\text{C}/\text{W}$, $R_{sa} = 2.5\text{ }^{\circ}\text{C}/\text{W}$ and $T_{air} = 30\text{ }^{\circ}\text{C}$, the calculated peak junction temperature was 67°C . In reality the safety factor should be taken into account. It is necessary to introduce the forced air cooling system for safety reason.

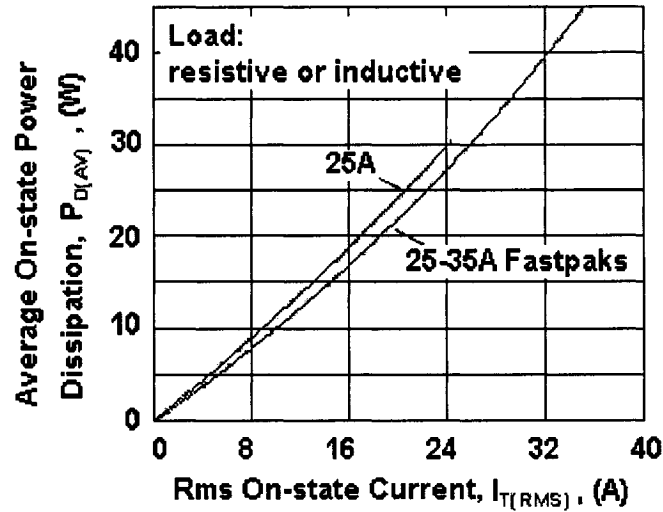


Figure 3.6 Power dissipation vs. on-state current (Source: Teccor Electronics, 2003)

The cooling air picked up the heat and its temperature rose. This might affect the cooling of the components down stream. In this design, the down stream components were the high voltage transformer, the filament transformer, and the magnetron. The temperature rise, ΔT , could be estimated from the following formula (Finney, 1980):

$$\Delta T = \frac{K_1 P_{loss}}{Q_{air}} \quad (3.4)$$

where,

Q_{air} = air flow rate (m^3/s)

P_{loss} = average power loss (W)

ΔT = temperature rise ($^{\circ}\text{C}$)

K_1 = conversion factor ($m^3/s/W$)

In the proposed design the heatsink was made from a flat piece of aluminum, with a thickness of 1.5mm, for providing less mounting torques, otherwise it might cause mechanical damage to the silicon wafer of the stud mounted thyristor. The heatsink was connected with the thyristor through the bolt and nuts. The cooling area of sink was $3000mm^2$. An air blower was chosen such that, in addition to cooling heat sink, it could also cool high voltage and filament transformers, and the magnetron.

3.3.2.6 Hysteresis Free Unit

In an RC oscillator, at the beginning of each cycle, the voltage acting on the capacitor keeps increasing until the diac is turned on; after that the capacitor voltage dropped. Each time this voltage might drop to a different value; this phenomenon is called hysteresis effect. Hysteresis causes the variation of the conduction time of the triac. Hysteresis free circuit could eliminate this unwanted effect such that each time the capacitor is set to the same initial condition. In the proposed circuit, the hysteresis free unit was created by using combinations of resistors and diodes.

3.3.2.7 RFI Filter

If the triac is used for fast switching at a high voltage level, unwanted electrical signals will be produced. These unwanted signals may cause radio frequency interference (RFI) so that the electromagnetic compatibility (EMC) may be lost. The effects of RFI can be minimized by a RFI filter which consists of an inductor in series to limit the current rate of rise and a capacitor in parallel to filter high frequency signals. For the given task, the RFI effect was negligible.

3.3.2.8 Control System for Power Regulator

The control system for a power regulator can take the forms of open-loop control

or close-loop control. In an open-loop there is no feedback of the output. In a close-loop the controlled variables, such as temperature, is detected and adjusted to the desired values. The control system for the proposed power regulator was by means of open-loop control. The resistance of the potentiometer in the RC oscillator was adjusted manually.

3.3.2.9 Summary

The proposed triac phase-controlled power regulator was developed based on phase control principle. Voltage applied to the high voltage (HV) transformer was adjusted by the fast switching operation of a triac. The triac was triggered (switched) 120 times per second. Triggering was realized by the diac. Triac conduction time was regulated by a RC oscillator. Open-loop control strategy was applied in this design. The variable output voltage was obtained by manually adjusting the resistance value of the potentiometer. Snubber, heat sink and hysteresis unit were introduced to improve the performance of the regulator. Figure 3.7 shows the block diagram of the proposed power regulator. The photograph of the regulator is illustrated in Figure 3.8.

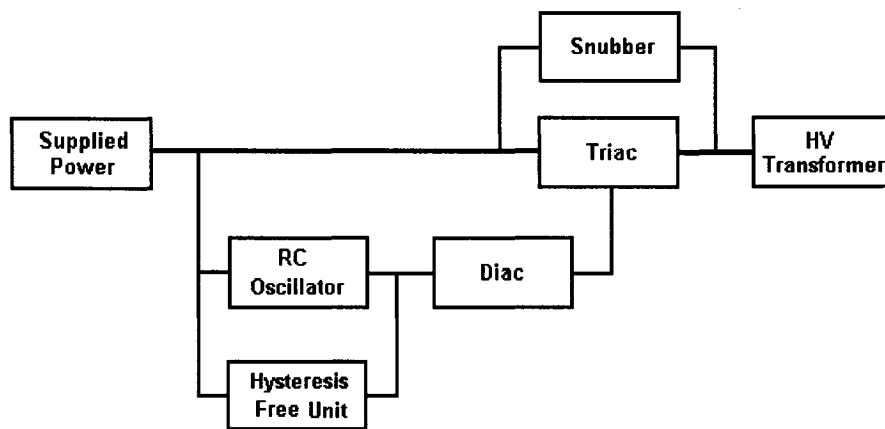


Figure 3.7 Block diagram of proposed triac power regulator

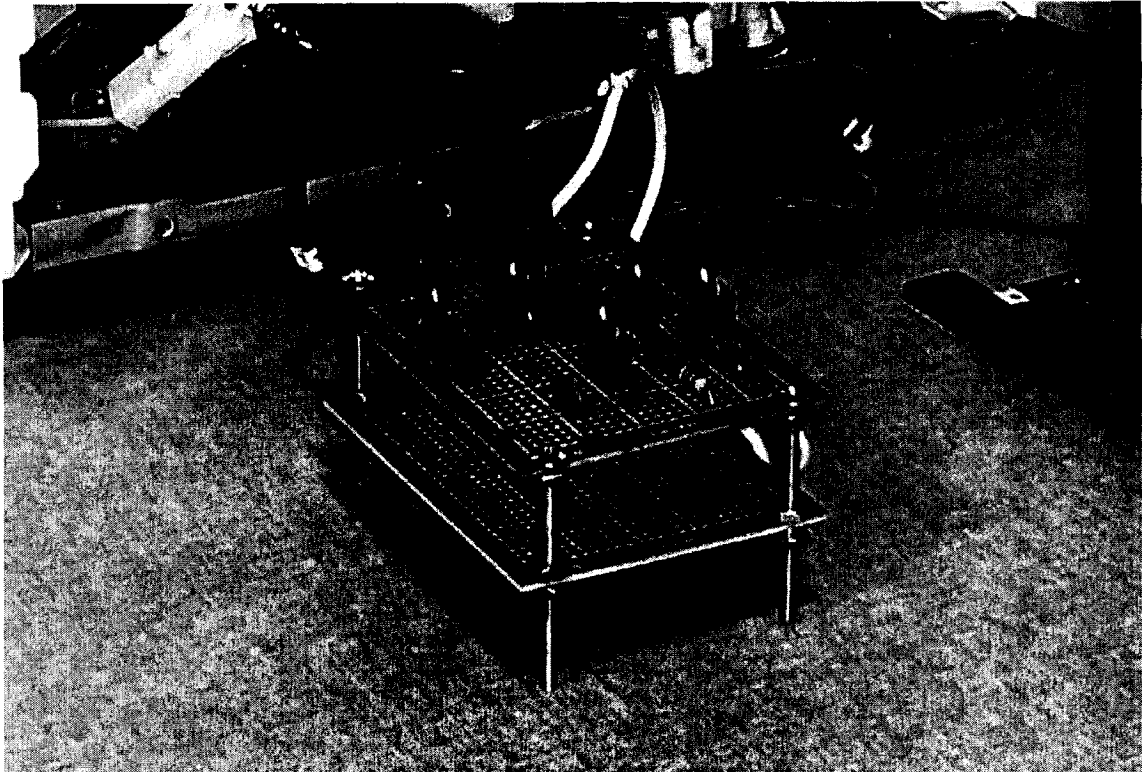


Figure 3.8 Photograph of the proposed triac power regulator

3.4 Modification of Original Electrical Circuit

The main components in the original electrical circuit included a filter, a cycle controller composed of a switch and a timer, a high voltage transformer, a filament transformer, a voltage doubler and a magnetron. Figure 3.9(a) shows the block diagram of the original electrical circuit.

In the original electrical circuit, the filament transformer and the high voltage transformer shared same power source. The filament emitted sufficient electrons to generate microwaves because the supplied voltage was always at its rated value as long as the circuit was turned on. However, when the power supply was phase-controlled, the input voltage became variable, and the filament was unable to produce enough electrons. For keeping the filament functioning a new filament transformer which had its own power source was introduced to replace the original one.

The same situation as the filament transformer happened to the existing cooling

fan. The variable input voltage resulted in the pulsating of airflow. In this study an additional air blower was brought in for cooling two transformers and magnetron when phase controller was in use. An extra application of the blower was to cool the triac.

The proposed triac phase-controlled power regulator was connected in series with the original integral cycle-controlled power regulator. The phase controller was located between the existing cycle controller and the magnetron. For safety reason, the existing electrical circuit, the introduced filament transformer, and the air blower were all connected to the same ground. Figure 3.9(b) shows the block diagrams of modified electrical circuit. Figure 3.10 shows the photograph of the modified electrical circuit.

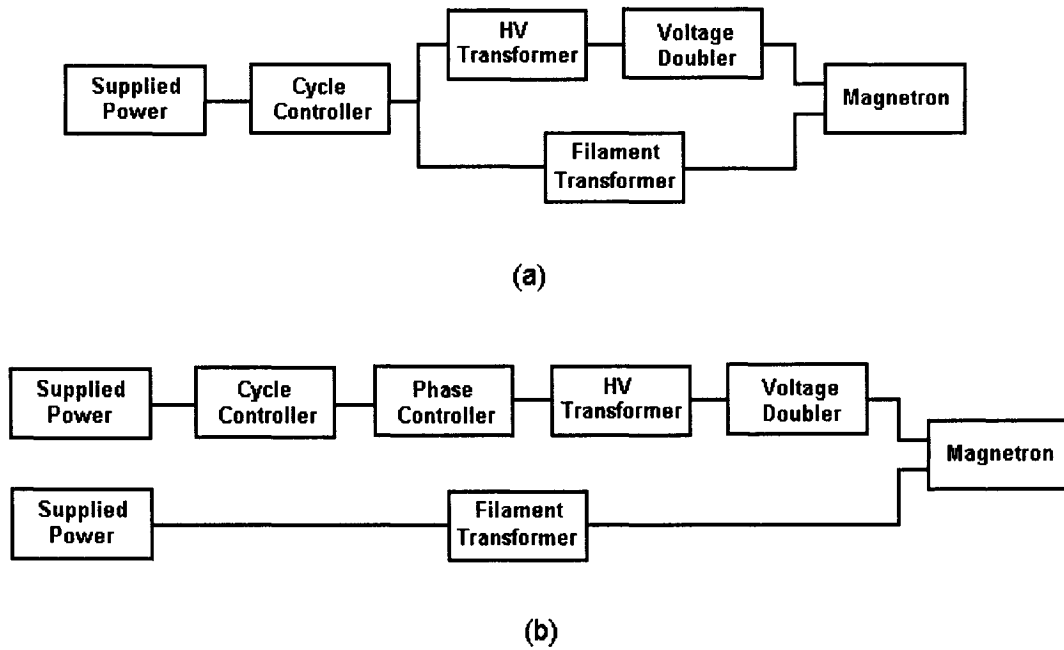


Figure 3.9 Block diagrams of (a) original circuit, (b) modified circuit

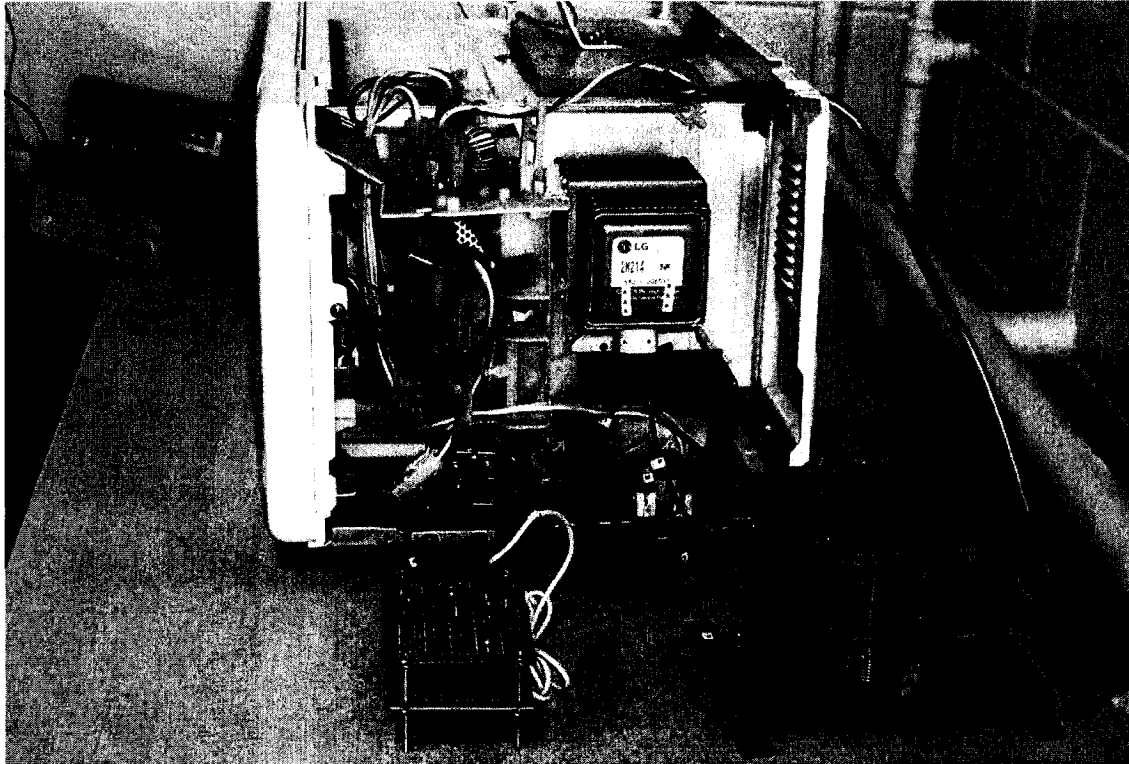


Figure 3.10 Photograph of the modified electrical circuit showing proposed triac phase controller and filament transformer

3.5 Instrumentation, Measurements and Control

In calorimetric measurement, the measured parameters were sample volume, sample initial and final temperatures. The sample volume was measured using the Teflon and Pyrex beakers. The initial and final temperatures were recorded with a K-type thermocouple.

In drying study, the monitored parameters included inlet air temperature, modulated air temperature, sample weight, sample temperature, and air velocity through the bottom of sample holder. The inlet and modulated air temperatures were recorded with K-type thermocouples. Figure 3.1 shows the locations where the temperatures were recorded. Modulated air temperature can be set and adjusted up to 60°C. A PID controller was used to control the supply power to heater coils to keep the modulated air temperature at set point. Modulated air velocity through the sample holder was calibrated

through the measurement of outlet air velocity. The sample weight was continuously monitored during each run through a strain gauge which was located on the top of the cavity and attached to the sample holder. The temperature at the center of sample was measured using a digital fiber optic thermometer (NoEMI-TS, Nortec Fiberopic Inc, Canada). Inlet and modulated air temperatures, and instantaneous weight data were recorded by a data acquisition system (HP34970A – Data Acquisition/Switch Unit, Hewlett-Packard, USA). A computer program was written in HPVEE to monitor the drying process.

The power supply to magnetron was controlled either by a triac phase-controlled power regulator or by an integral cycle-controlled power regulator. When the cycle controller is in use, ten power levels from 10% to 100% of maximum power level can be selected through the existing control panel. For the phase controller the power can be set continuously at any value from 0% to 100% of rated power level through adjusted output voltage of the controller (voltage applied to high voltage transformer). Open-loop control strategy was adopted in both control methods; hence, there was no feed back of controlled variables, and power supply to magnetron was preset manually.

3.6 Calorimetric Test

The sample used in calorimetric tests was the tap water with the initial temperature of $22\pm 3^{\circ}\text{C}$. Tap water with a fixed volume was poured into Teflon or Pyrex beakers. The water was stirred before the initial temperature was measured. The beaker was put on the floor of the microwave oven. After the designated heating time was over the beaker was taken out, the water was stirred and the final temperature was read. Each experimental run was replicated twice.

3.7 Drying Process

The drying tests were conducted in the batch mode. Potato (unknown cultivar)

purchased from a local grocery store was used for the experiments. Materials were stored in a storage room set at an air temperature of 4°C. Before drying trial, the materials were taken out and kept at room temperature for about 24 hours for thermal equilibrium. The initial moisture content of samples were determined in an oven at a temperature of 105°C for 24 hours following the procedure prescribed by ASAE standards (ASAE, 1991). The initial moisture content was 77.5% (wet basis) or 3.44 kg/kg (dry basis) for potato. Before the first run of each day, the drying setup was subjected to microwave leakage checking and system preheating. Tap water with preset volume in the glass beakers was placed in the cavity and microwave oven was turned on (full power) for leakage checking. A microwave leakage detector (DJF-2000, Nankai, China) was used for monitoring the leakage. Hot air was used to preheat the setup for 20 minutes with preset temperature and air velocity for thermal stabilization.

Samples were prepared before each experimental run. Potatoes were peeled and cut into cubes of 10×10×10mm. All samples were taken from the center medulla region of the potato tuber for a more uniform cell structure (Khraisheh et al., 2000). The sample cubes were immediately soaked in tap water (approximately 16°C) to prevent browning before all cubes were cut (Prothon et al., 2001). Samples were evenly spaced and placed as a single layer on the base of the sample holder.

As a first step of each run, the data acquisition system was switched on. The air velocity and modulated air temperature were then set to the desired value. A sample of 50 grams was used for each run. Sample center temperature was monitored. During each trial, inlet air and modulated air temperature, sample weight and sample temperature were recorded continuously by the data acquisition system. The drying process was finished when the sample reached the moisture content of 10% (wet basis), or 0.11kg/kg (dry basis). The air was introduced for taking away the evaporated water and for surface cooling reasons. Since the ambient air temperature varied from 14 to 22°C, a modulated air temperature of 25 °C was used during all drying tests. The values of operational

parameters are shown in Table 3.3.

Table 3.3 Operational parameter during microwave/air (MWA) drying

Parameter	Levels
MW power density, P (Power level, PL)	0.994W/g (10%), 1.988W/g (20%)
Air velocity, V_A	0.5m/s, 1.5 m/s
Ambient temperature, T_{amb}	14 - 22°C
Modulated air temperature, T_{air}	25°C
Sample weight, W_s	50g
Sample initial moisture content, x_i , or X_i	77.5% (wet basis), or 3.44kg/kg (dry basis)
Sample final moisture content, x_f , or X_f	10% (wet basis), or 0.11kg/kg (dry basis)

3.8 Quality Evaluation

3.8.1 Rehydration Capacity

Rehydration tests were performed by immersing a weighed sample into water at 20°C for 120minutes. After that, the samples were drained over a mesh for 30seconds and quickly blotted with paper towels and weighed. Rehydration capacity was expressed as a percentage of water gained by noting the difference in sample weight from before and after rehydration (Sanga, 2002):

$$WG(\%) = \frac{W_{st} - W_{s0}}{W_{s0}} \times 100 \quad (3.5)$$

where:

WG = water gained (%)

W_{st} = sample weight at time t during rehydration (g)

W_{s0} = sample weight at time zero during rehydration (g)

3.8.2 Colour Analysis

A chromameter (CR-300X, Minolta Camera Co. Ltd., Japan) with a 5 mm diameter measuring area was used for surface colour measurements. The instrument was calibrated on a standard white plate ($L^* = 98.28$, $a^* = -0.05$, and $b^* = 2.32$). The L^* coordinate ranged from 0 (black) to 100 (white), the a^* coordinate indicated red-purple colour (positive value) or bluish-green colour (negative value), and the b^* coordinate indicated yellow colour (positive value) or blue colour (negative value) (McGuire, 1992). In this study, the reading was done on the external surface of the sample; the mean of three readings at random locations on the sample was reported. Each reading gave three different coordinates L^* , a^* , and b^* .

3.8.3 Sensory Evaluation

The dried samples were subjected to evaluation by a panel of six untrained judges for visual appearance, taste, and textural consistency, etc. The results were expressed in the categories of unsatisfactory, poor, neutral, good, and satisfactory.

3.9 Statistical Analysis

Each experimental run was replicated twice and a mean value was reported. Data collected through the tests were subjected to analysis of variance (ANOVA). Differences were identified as significant and insignificant with respect to a significance level of 0.05 ($P < 0.05$) applied in all cases.

CHAPTER IV. RESULTS AND DISCUSSION

4.1 System Performance

4.1.1 Calibration of Maximum Microwave Output Power

The nominal power of existing microwave oven was 700 W as given by the manufacturer. It is necessary to determine the actual output power which is different from the declared capacity by the manufacturers.

Calorimetric method is widely used for the measurement of output power in a microwave oven both by manufacturers and by researchers (Pandit and Prasad, 2003; Costa et al., 2001; Sharma and Prasad, 2001; Gallawa, 1999; Khraisheh, 1997; Puacz and Szahun, 1996; Kingston and Jassie, 1988a; Schiffmann, 1987), and was adopted in this study. The sample used in this experiment was the tap water with the initial temperature of $22\pm 3^\circ\text{C}$. Tap water of 1000g was poured into a Teflon beaker. The water was stirred before noting the initial temperature. The beaker was placed on the center of the floor of the microwave oven and heated for a designated time period. Then the beaker was taken out, the water was stirred and the final temperature was read. Both initial and final temperatures were recorded using a K type thermocouple. The absorbed power was calculated using the following equation (Neas and Collins. 1988),

$$P_{ab} = \frac{KC_p W_s \Delta T}{t} \quad (4.1)$$

where:

P_{ab} = absorbed microwave power by water (W)

K = conversion factor (J/cal)

C_p = heat capacity (cal /g / $^\circ\text{C}$)

W_s = sample weight (g)

ΔT = temperature rise ($^\circ\text{C}$)

t = heating time (s)

In all the tests, the input power was set at 100% rated level and phase controller was not used in this calibration process. Each run was carried out in triplicate and the mean value was noted. The source input voltage was 120V at 60 Hz. The experimental results show the maximum output power of existing microwave oven to be 497 W, which is 71% of nominal value of 700W.

According to Gallawa (1999) and Khrasisheh (1997), the variance between claimed and recorded powers is caused by several reasons such as the aging of the magnetron, the overheating of the filament, and the numerous methods available for power measurements. In the current tests, each run only lasted for a short period of time, this difference between claimed and recorded powers (degradation of microwave power) may be explained due to the aging of the magnetron, not the overheating of the filament.

4.1.2 Determination of Distribution of Microwave Field Inside Cavity

Microwaves are emitted in an irregular array in most microwave ovens, producing hot and cold regions in the cavity (Davis et al., 1997). Therefore it is desirable to identify the hot and cold spots before conducting the drying tests. The calorimetric technique (Chen et al., 1993) was employed in the proposed experiments to determine the distribution patterns. Other technique such as neon bulb method (Login et al., 1996), in which the bulbs glowed brightly to indicate the locations of the hot spots, cannot give the quantitative power values.

Nine Pyrex beakers were placed simultaneously on the floor of the cavity during each run. Figure 4.1(a) shows the locations of the nine beakers. Each beaker contained 200g tap water with an initial temperature of $22\pm 3^{\circ}\text{C}$. The initial and final water temperatures in each beaker were measured using the same procedures described in §4.1.1. Temperature measurements were made as quickly as possible to minimize the temperature drop. Absorbed power was computed using equation (4.1). The power distribution was expressed as percentage of absorbed microwave power at each location

to the total power absorbed and calculated by,

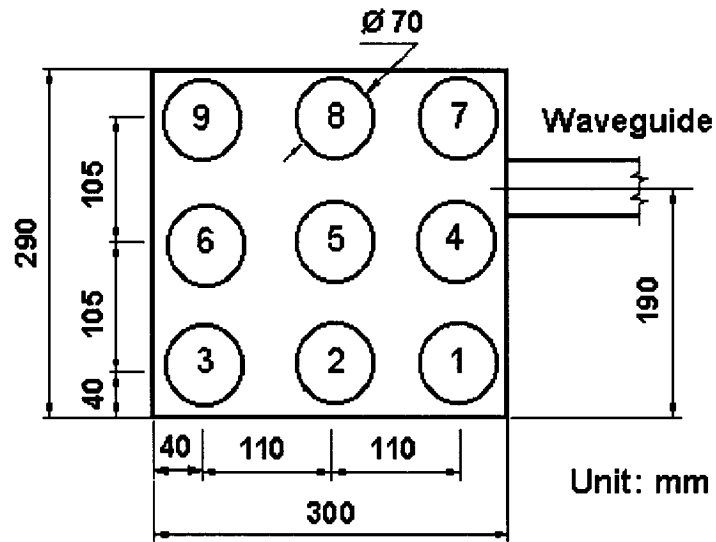
$$PA (\%) = \frac{P_{ab,i}}{\sum_{i=1}^9 P_{ab,i}} \times 100 \quad (4.2)$$

where:

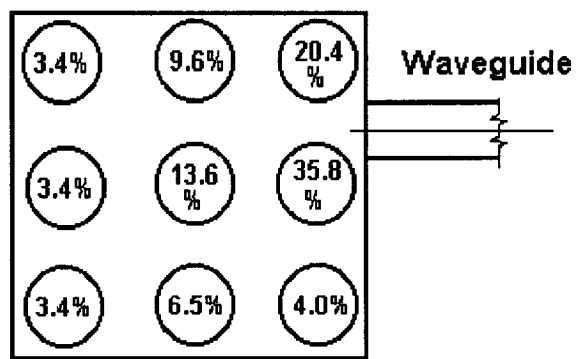
PA = percentage of absorbed microwave power (%)

$P_{ab,i}$ = absorbed microwave power by sample i (W)

Σ = summation operator



(a)



(b)

Figure 4.1 Top view of microwave cavity showing (a) measurement locations, (b) microwave power distribution at different locations

During each test, the input power was set at full level and phase controller was not employed. Each run was carried out in triplicate and the mean temperature value was noted. The calculated results based on equation (4.2) are shown in Figure 4.1 (b). Power distribution was uneven and, the hot spots (locations #4, #5, #7 and #8) and cold spots (locations #1, #2, #3, #6, and #9) were created inside cavity. The absorbed power at the hottest spot was ten times (35.8%) to that at the coldest spot (3.4%). The power distribution was marked by the decreasing of power value with the increasing of distance to the microwave entrance, from 20.4% (#7) to 9.6 % (#8) and 3.4% (#9) along the back row; and from 35.8% (#4) to 13.6% (#5) and 3.4% (#6) along the middle row.

It can also be noted in Figure 4.1(b) that the absorbed power at the corner was much less than expected. Compared power values at locations #4 and #7, both had the nearest distances to the microwave entry, the power at #7 was only 57% of that at #4. Same phenomenon was found at location #1 which was closer to the microwave entrance compared to #2, but the power was less at #1 than #2 by 62.5%.

Kingston and Jassie (1988b) found that the microwave energy field is not homogeneous enough for samples at different positions in the cavity to achieve reproducible and uniform energy exposure. Even when mode stirrers are used to homogenize the field, temperature differences of as much as 50% can be observed in identical vessels placed at different locations within the microwave cavity.

Strategies should be employed, if uniform distribution of microwave field inside cavity is desired, which may include,

- Introduction of mode stirrers and turntables,
- Application of multiple magnetrons and cavities,
- Improvement of cavity design, such as dimensions and geometry,
- Application of continuous processing unit, if possible.

In the current drying study, the size of the sample holder is relatively small compared to the cavity; it is reasonable to expect that the microwave field nonuniformity

is not too severe inside the area where the sample holder is located.

4.1.3 Preliminary Studies on a Commercial Triac Phase Controller

The objective of the preliminary studies was to determine the factors that should be taken into account in the development of a new power regulator. In this study, three circuits named circuits #1, #2, and #3 were built based on a commercial circuit (Figure 3.3) of Teccor Electronics Company of USA.

The circuit #1 with the triac current rating of 10A was connected in series to a 40W incandescent lamp that was a resistive load. Normally the turn-on surge current for an incandescent lamp is 12 to 18 times the steady state current and this may cause failure of the circuit. But there was no such problem in the circuit #1 as the rating current of the triac was as high as 10 A. The waveform of load current corresponded to that of the load voltage. With the adjustment of the resistance of the potentiometer (R_1), the dimmer and lighter of the light in the incandescent lamp were observed; which implied the circuit can be used for a resistive load. No further tests and analyses were done about this resistive load.

The circuit #2 with the triac current rating of 10A was connected to the primary winding of the transformer of existing microwave oven. The calculated root-mean-square (rms) load current flowing through the high voltage (HV) transformer is 8.2A. Tap water contained in a Teflon beaker load was put into microwave oven for calorimetric measurements. Due to overheating, the triac burnt out after intermittently working for dozens of minutes. No reasonable experimental data were recorded.

The circuit #3 with the triac current rating of 20A was connected to the primary winding of the transformer of existing microwave oven. In all tests, the original integral cycle-controlled power regulator was set at full power level. A new filament transformer which had its own power source replaced the original one. The output voltage of the phase controller (voltage to HV transformer) was set by manually adjusting the resistance

values of potentiometer in the RC oscillator. Several levels of voltage to HV transformer were preset for different trials. The sample used in this experiment was the tap water of 1000g with an initial temperature of $22\pm 3^\circ\text{C}$. Calorimetric method described in §4.1.1 was used for the measurements. Each run was carried out in triplicate and the mean value was noted. Figure 4.2 shows the experimental results. It was found that the absorbed power by the tap water increased with the increasing of the preset applied voltages to HV transformer. But the maximum absorbed power was less than half of the nominal power which implied that the triac phase-controlled power regulator did not function properly. Besides, overheating of triac was observed.

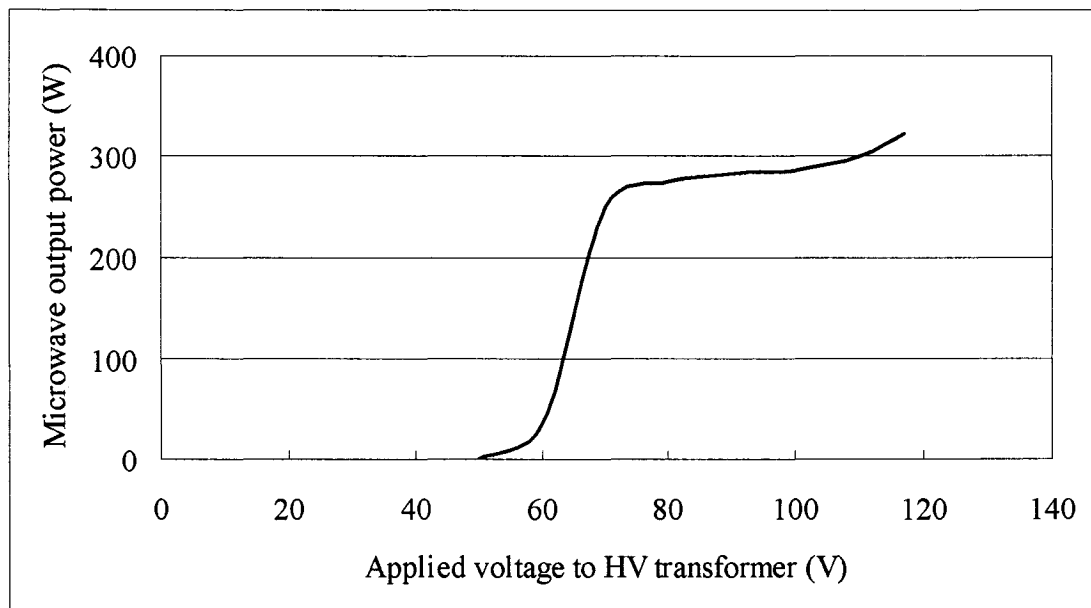


Figure 4.2 Microwave output power versus applied voltage to HV transformer for preliminary study on a phase controller

Mazda (1993) listed four main sources of power losses within a semiconductor. One of them was the switching loss that occurs during turn-on or turn-off of the device. The loss can become appreciable when the device is being operated at high frequencies. For the inductive load, Williams (1992) stated that the voltage spikes generated by

inductive loads at turn-off might generate high-energy content. Both the voltage spike and its associated energy may well be outside the capabilities of the switching device and may cause excessive temperature and device failure. The results of preliminary studies on the triac circuits #2 and #3 corresponded to those discussed in the above literature.

The preliminary studies showed that for a triac phase controller to function properly several factors must be taken into account during design, they are:

- Load characteristics in the selection of thyristors,
- Triggering strategy,
- Transient current and voltage,
- Extent of current and voltage,
- Dissipation of heat and cooling of device.

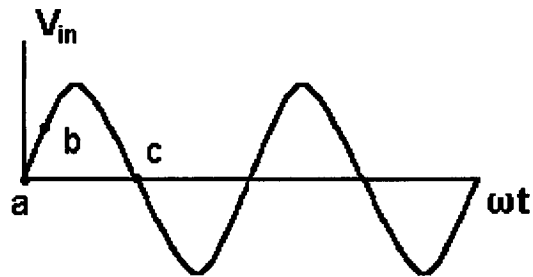
4.1.4 Evaluation of New Triac Phase-controlled Power Regulator

4.1.4.1 Physical Description of Phase Control Process

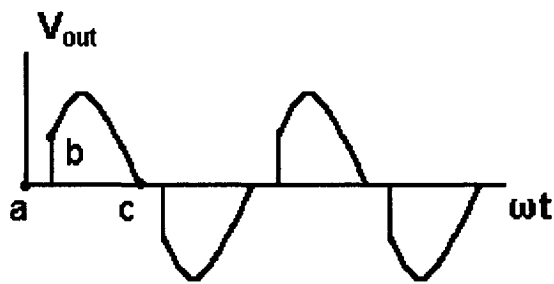
Normally the triac is in OFF condition, that is, all current flowing through the main circuit is blocked by the triac (Figure 3.7). At the beginning, the positive half cycle of the source voltage (point *a* in Figure 4.3) starts to charge the RC oscillator. When the voltage of the RC oscillator reaches the diac break-over voltage ($V_{BO} = +30V$), the diac conducts. The forward gate current flows through diac and increases rapidly while the voltage across the diac decreases slightly. After forward gate current reaches the required value ($I_{GT} = +50mA$) of the triac, the triac is switched on. The positive half cycle of the source voltage is applied to HV transformer (point *b* in Figure 4.3). Assume there is a 0° phase shift between primary and secondary windings in the transformer; the amplified output voltage is stored in the voltage doubler and no voltage exerts on the magnetron during this half cycle.

After the turn-on of triac, the gate current drops but the triac is still in the positive ON state. When the gate current becomes zero, triac continuous to conduct as long as the

main current is larger than the holding current ($I_H = +100\text{mA}$). When the main current drops below the holding current, which is near the end of positive half cycle of the input source voltage, the triac is switched off.



(a)



(b)

Figure 4.3 Patterns of voltage waveforms (a) input source voltage, (b) voltage applied to HV transformer with the omitting of transient voltage

The physical process during the negative half cycle is exactly the same as that during the positive half cycle. The RC oscillator is charged by the negative half cycle of the voltage source. When the reverse break over voltage is reached, the negative gate current flows through the diac. The triac is conducted after the gate current achieves the required value. The negative half cycle of the input source voltage is applied to the

transformer. The amplified voltage from the transformer is added to the voltage previously stored in the voltage doubler. The sum voltage is applied to the magnetron to generate microwave power.

4.1.4.2 Performance of New Triac Phase Controller

From the electrical point of view, the worthwhile parameters for performance evaluation include current, voltage and power. Direct electrical measurements on a phase-controlled circuit are not easy work due to the unusual current and voltage waveforms (Finney, 1980). The high voltage transformer adds transient contents and makes these waveforms further harmonic. To make things even more complex, the peak voltage on the secondary winding of the transformer is nearly 6000V. Special kinds of instruments and careful measurement are required for accurate results. Since direct electrical measurements and analysis of the triac phase controller are beyond the scope of current study, the calorimetric method was introduced as an alternative approach for evaluation of the proposed triac phase controller.

During the tests, the phase controller was connected to the primary winding loop and in series to the existing cycle controller. The output power of cycle controller was fixed at 100% power level. The original filament transformer was replaced by a new one which had a separate power source. The output voltage of the phase controller (voltage to HV transformer) was measured and manually adjusted through the potentiometer in the RC oscillator. The voltage to HV transformer was preset from zero to maximum value, in increments of 5V, for different tests. Calorimetric technique illustrated in §4.1.1 was used for the measurements. The sample was tap water of 1000g with an initial temperature of $22\pm 3^{\circ}\text{C}$. The source voltage was 120V at 60Hz.

Based on the measurements of initial and final temperatures, the output power was calculated. Figure 4.4 shows the variation of the output microwave power with applied voltage to HV transformer. As expected the microwave power absorbed by tap water

increases with applied voltage to HV transformer. The power versus voltage curve can be divided into three different zones, a slow rise of output power at voltage above 50V, followed by a rapid jump between 80V to 100V, after which the curve becomes relatively flat. The maximum microwave output power was found to be 492W. Compared to 497W reported in §4.1.1 when the phase controller was not in use, the difference shows that 5W power was dissipated in the phase controller. It is reasonable to expect majority of the 5W power is consumed in the triac which converted to heat. The corresponding voltage to HV transformer is 117V when 492W maximum power is reached, which means there is a 3V drop of voltage in the circuit between power source and HV transformer. No temperature rise of sample was recorded when the voltage to HV transformer was below 50V. This is because the electric field inside magnetron became very weak such that the resonance of electrons could not happen and, as a result, no microwave energy was generated. Similar pattern for microwave output power changes with supplied voltage to HV transformer was observed by Sun et al. (2000).

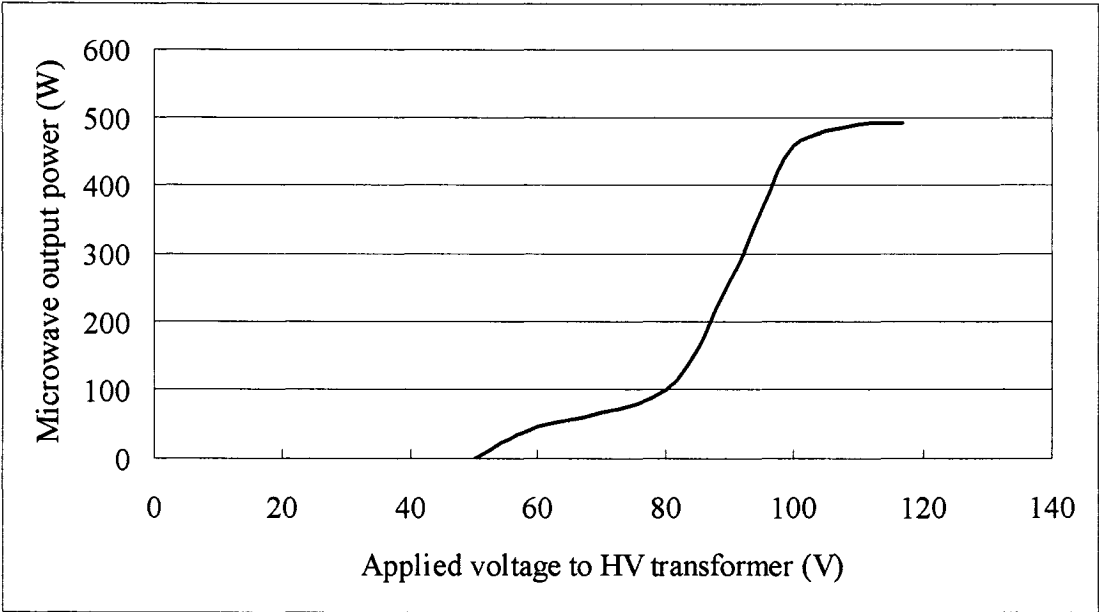


Figure 4.4 Microwave output power versus applied voltage to HV transformer for evaluation of new phase controller

Above experimental results show that the proposed triac phase controller can be used for precisely regulating microwave power. More accurate temperature control could be realized compared to power cycle control method. It is also reasonable to expect higher power efficiency in phase control process than that in resistive control process, because the latter process always consumes full power level no matter what output power level is actually used.

4.2 Drying Modes

The microwave dryer in the current study was operated in two drying modes as described below:

- Phase-controlled microwave/air (MWA) drying – Electrical power supply was controlled by a triac phase controller. The microwave and air were introduced simultaneously through whole drying process. The power cycle controller was set to full power level when this drying mode was employed.
- Cycle-controlled microwave/air (MWA) drying – Electrical power supply was controlled by a cycle controller. The microwave and air were introduced simultaneously through whole drying process. The power phase controller was removed from the circuit when this drying mode was employed.

4.3 Drying Characteristics

The influence of power density, and air velocity were examined in individual drying mode. Comparison of two drying modes was performed with respect to drying kinetics and material temperature.

4.3.1 Phase-controlled MWA Drying

Typical drying curves of potatoes under different MW power densities and air velocities are shown in Figures 4.5, 4.6, 4.9, 4.10, 4.11, and 4.12, respectively.

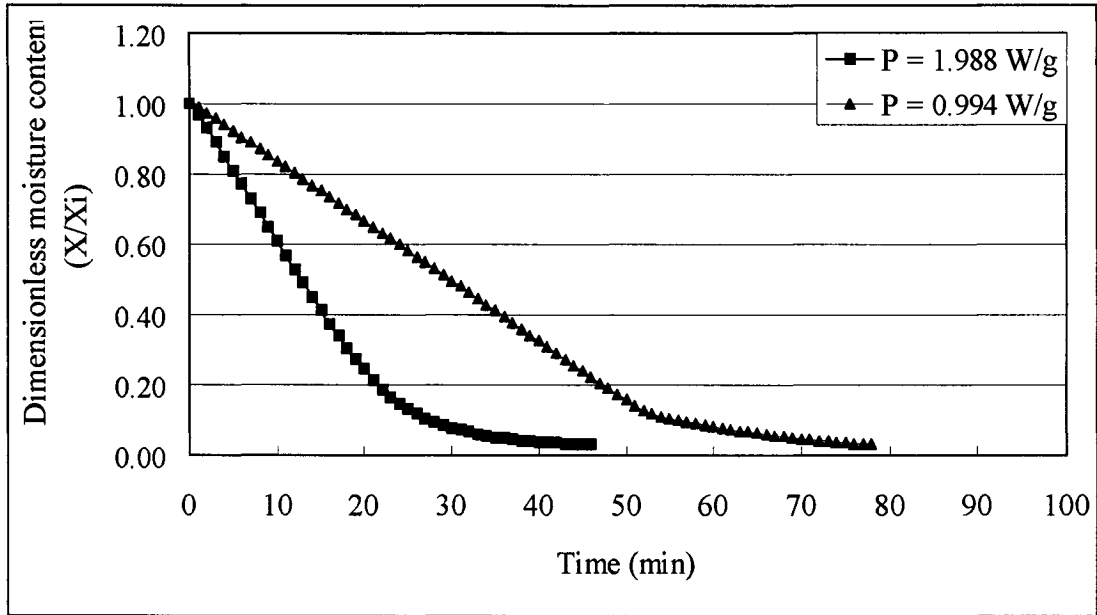


Figure 4.5 Dimensionless moisture content during phase-controlled MWA drying, air temperature at 25°C and air velocity at 0.5m/s

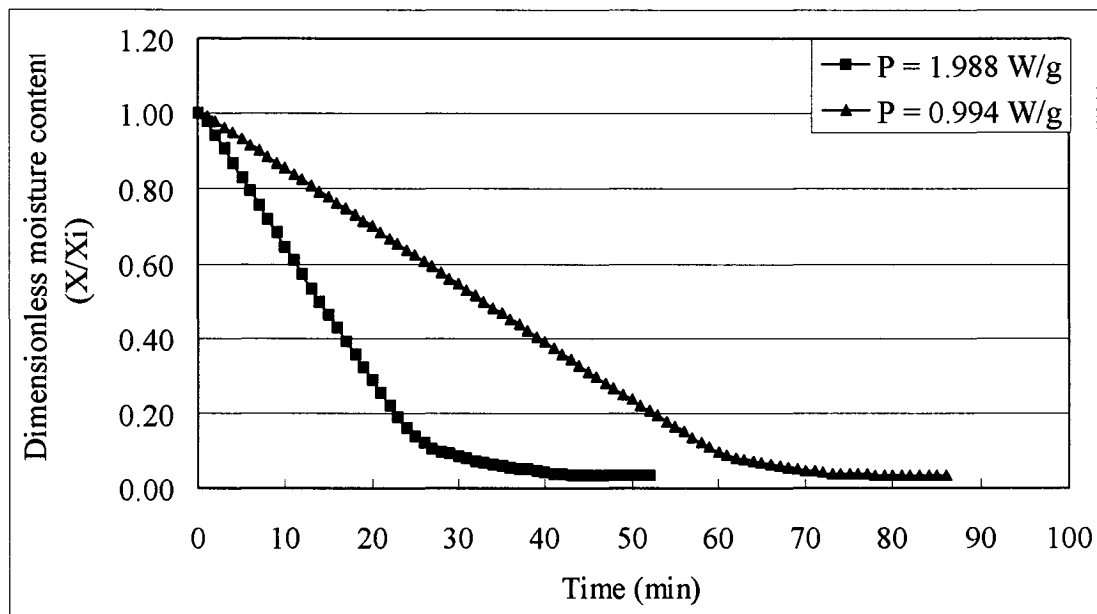


Figure 4.6 Dimensionless moisture content during phase-controlled MWA drying, air temperature at 25°C and air velocity at 1.5m/s

The dimensionless moisture content is expressed by,

$$MC_{dl} = \frac{X}{X_i} \quad (4.3)$$

where:

MC_{dl} = dimensionless moisture content

X = sample moisture content (kg/kg, dry basis)

X_i = sample initial moisture content (kg/kg, dry basis)

The dimensionless content and drying rate curves resembled roughly a typical drying curve with three zones, a preheat period followed by a constant rate period, and at last, a falling rate period. Most moisture evaporated during constant drying rate period. The reason for the higher drying rate was that the sample had a high moisture content which possesses high dielectric loss, as a result, more microwave energy was absorbed by the material to drive the liquid into vapor. The drying rates became extremely low near the end of drying process, for instance, it took about 13 minutes to reach about a 5-point reduction (15 to 10%, wet basis) for drying at $P = 0.994$ W/g ($V_{air} = 0.5$ m/s). The lower drying rate during falling rate period was due to a decrease in dielectric loss caused by the reduced moisture content.

The MW power density appeared to have significant effect on phase-controlled MWA drying process. In all cases, the drying times increased with the decrease of MW power density. For example, at $V_{air} = 0.5$ m/s, the whole drying time decreased from 78 to 46 minutes when the power density increased from 0.994 to 1.988 W/g. This was because higher power density resulted in the high mass transfer driving force and sped up drying course. Besides, higher power density caused higher material temperature (Figures 4.13 and 4.14) and increased the rate of moisture evaporation. Note that at MW power density $P = 2.982$ W/g (PL = 30%) and above, the product had serious burnt spots due to higher product temperature which was over 100°C before drying process finished.

It is observed that the drying time was positively correlated with air velocity. That

is, an increase in air velocity would increase the drying time. For instance, at $P = 0.994$ W/g, the total drying time at $V_{\text{air}} = 0.5$ m/s and 1.5 m/s were 78 and 86 minutes (an increase of nearly 10%), respectively. While at $P = 1.988$ W/g the corresponding total drying times were 46 and 52 minutes, separately. This was mainly due to the faster cooling effect of higher air velocity which prolonged the drying time. Corresponding drying rate curves (Figures 4.9 to 4.12) further confirmed the effects of MW power density and air velocity.

4.3.2 Cycle-controlled MWA Drying

The cycle-controlled MWA drying characteristics of potatoes under different MW power densities and air velocities are illustrated in Figures 4.7 to 4.12. As the phase-controlled MWA drying process, these curves can be divided into three distinct regions, a preheat region, a constant rate region and, a falling rate region. As expected, during cycle-controlled MWA drying process, higher power density shortened the drying time and increased the drying rate. An increase of 42% in drying time was found at $V_{\text{air}} = 0.5$ m/s when MW power density reduced from 1.988 W/g to 0.994 W/g. The air velocity also exhibited its cooling effect which lengthened the processing time. The same phenomenon during microwave drying of potatoes was also observed by Lu et al. (1999) and Beke et al. (1997).

4.3.3 Phase-controlled MWA Drying versus Cycle-controlled MWA Drying

4.3.3.1 Drying Rate

Drying rate curves for drying of potatoes during two different drying modes for MW power densities $P = 0.994$ and 1.988 W/g at air velocities $V_{\text{air}} = 0.5$ m/s are shown in Figures 4.9 and 4.10, respectively. Corresponding drying rate curves at $V_{\text{air}} = 1.5$ m/s are shown in Figures 4.11 and 4.12, separately.

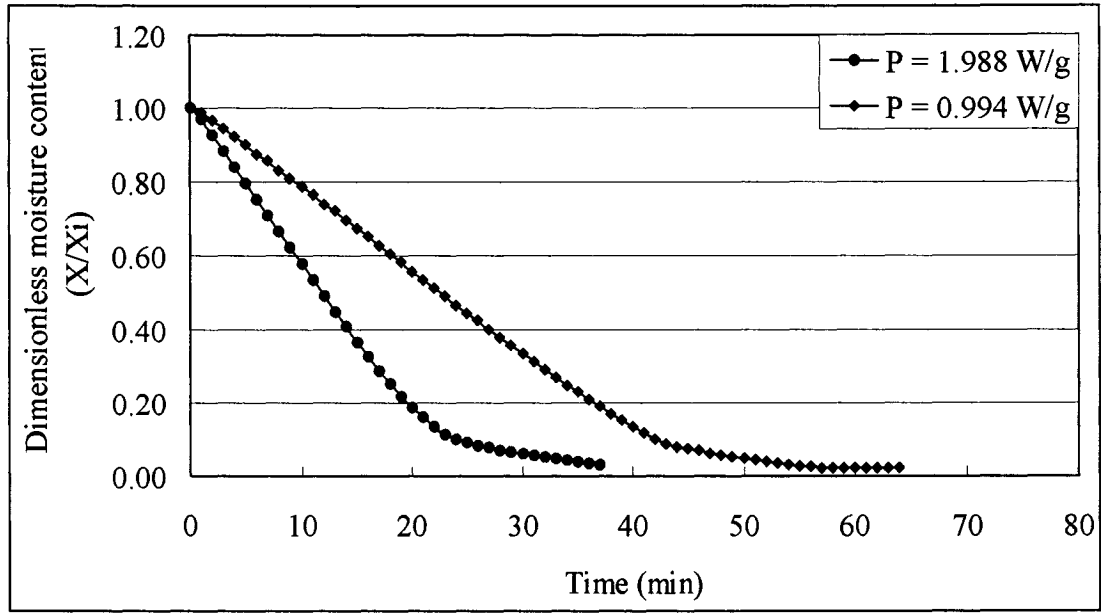


Figure 4.7 Dimensionless moisture content during cycle-controlled MWA drying, air temperature at 25°C and air velocity at 0.5m/s

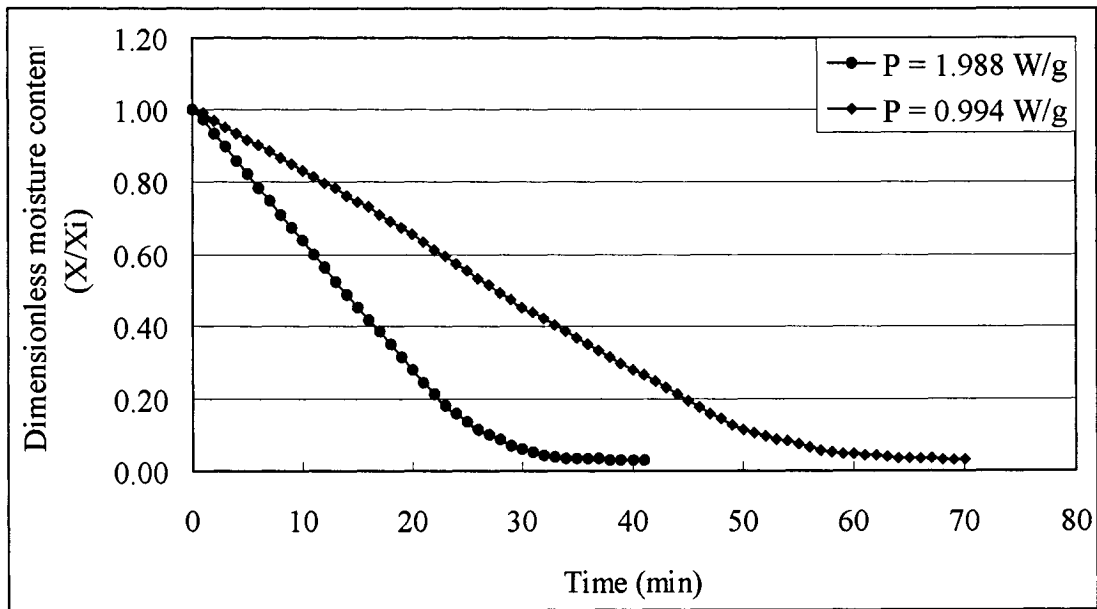


Figure 4.8 Dimensionless moisture content during cycle-controlled MWA drying, air temperature at 25°C and air velocity at 1.5m/s

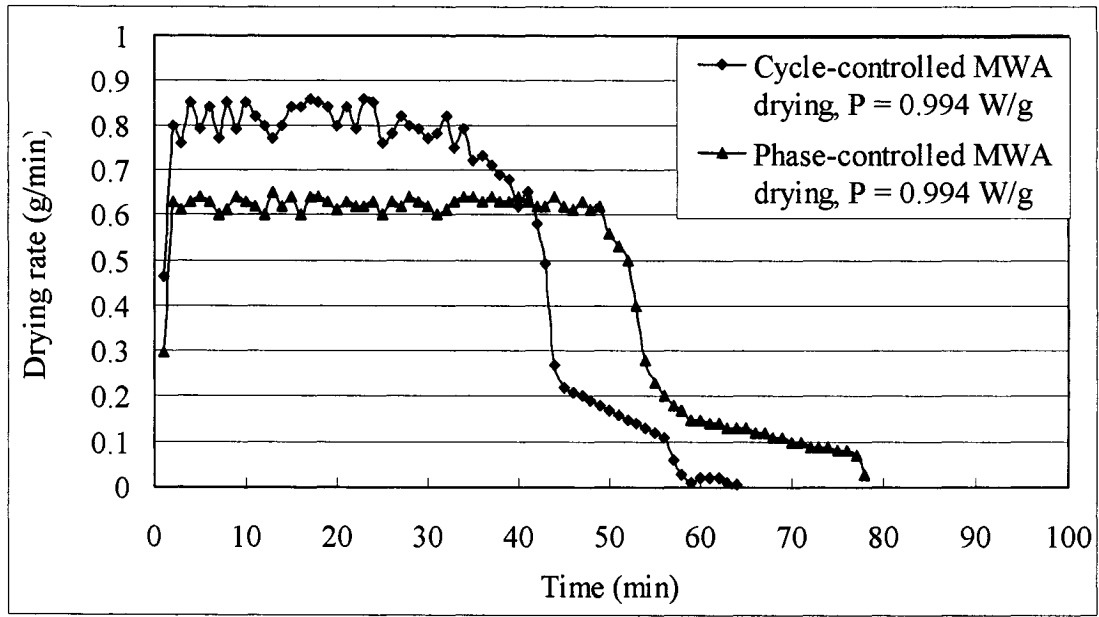


Figure 4.9 Drying rate during drying with power density of 0.994W/g, air temperature at 25°C and air velocity at 0.5m/s

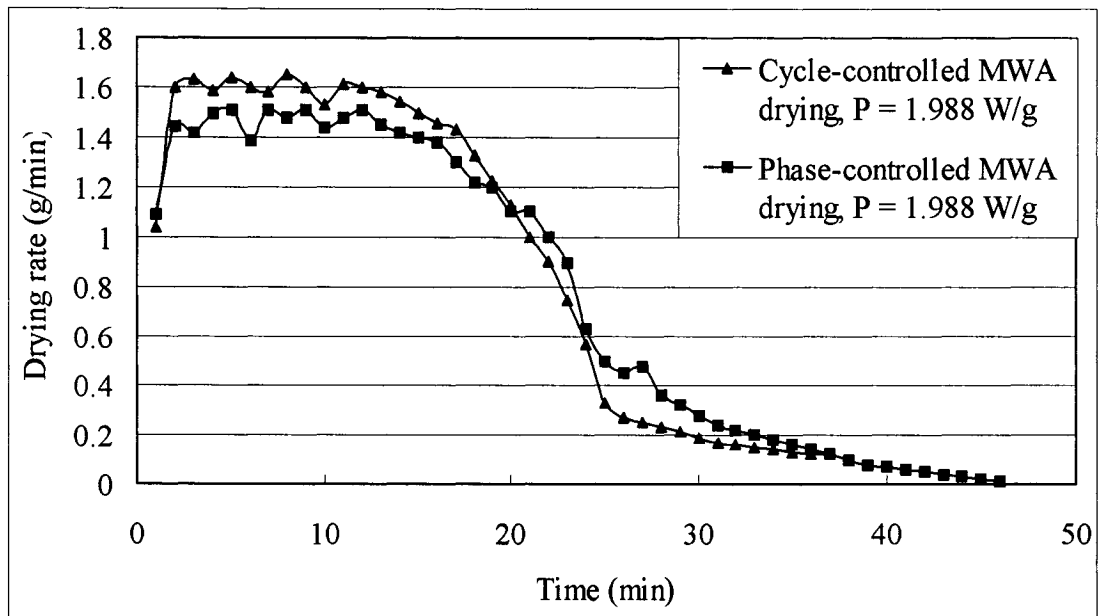


Figure 4.10 Drying rate during drying with power density of 1.988W/g, air temperature at 25°C and air velocity at 0.5m/s

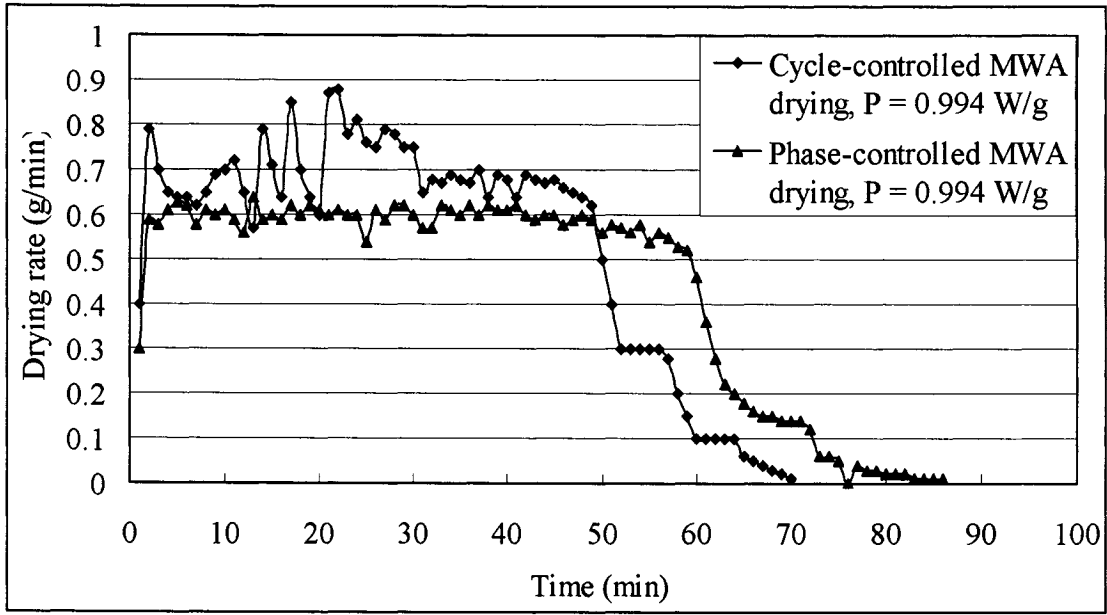


Figure 4.11 Drying rate during drying with power density of 0.994W/g, air temperature at 25°C and air velocity at 1.5m/s

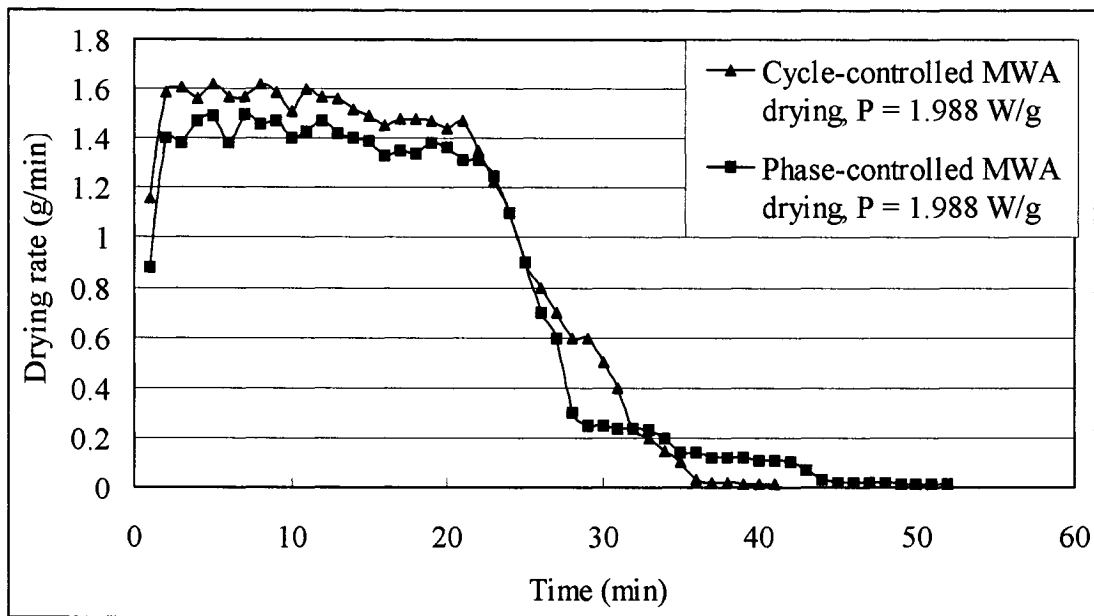


Figure 4.12 Drying rate during drying with power density of 1.988W/g, air temperature at 25°C and air velocity at 1.5m/s

In all cases the constant drying rates during cycle-controlled MWA drying are significantly ($P < 0.05$) higher than those during phase-controlled MWA drying. Table 4.1 gives the constant drying rate for various combinations of parameters.

Table 4.1 Constant drying rate during two given drying modes

Power density, W/g	Air velocity, m/s	Constant drying rate, g/min	
		Phase-controlled MWA drying	Cycle-controlled MWA drying
0.994	0.5	0.625	0.788
	1.5	0.593	0.699
1.988	0.5	1.457	1.571
	1.5	1.395	1.539

The reason that the higher drying rate obtained during cycle-controlled MWA drying process is that, although only 10 and 20% power levels were actually applied in this study, the materials always faced 100% power level through ON period of duty cycles. The 100% rated power produced intensive mass transfer driving force, and as a result, an enhanced temperature and a higher drying rate was established. In addition, the treated materials had relatively higher dielectric loss during constant drying rate period which had the capacity to absorb a higher level of microwave power, which further sped up the drying process. On the other hand, during phase-controlled MWA drying, the input electrical voltage waveform was chopped one time during each half cycle. The instant applied power was mild and driving force was relatively small.

The difference of drying rate in falling rate region was insignificant between the two drying modes. This result implied that the internal resistance to mass transfer became dominant when the moisture content was relatively low.

4.3.3.2 Material Internal Temperature

Figures 4.13 and 4.14 give the material internal temperature for drying of potatoes during two different drying modes for MW power densities $P = 0.994$ and 1.988 W/g at air velocities $V_{\text{air}} = 0.5$ m/s, respectively. Different patterns of temperature variation were observed between the two drying modes.

The temperature curve during cycle-controlled MWA drying could be roughly split into three different zones. At first, the temperature rose, first sharply and then gradually, to reach a peak value, which was 74.97 and 88.94 °C for MW power density of 0.994 and 1.988 W/g, respectively. The material temperature dropped slowly after reaching maximum value followed by a steady temperature period. As shown in drying rate curves (Figures 4.9 and 4.10), the first and second temperature zones approximately correspond to the constant drying rate region where most moisture loss occurred. On the other hand, two distinct zones were observed in temperature curve during phase-controlled MWA drying, a gradual temperature rising zone followed by a stable temperature zone, the first zone nearly matches the constant drying rate region.

The temperature fluctuations were recorded during cycle-controlled drying process, which corresponds to the ON and OFF periods of the duty cycles. These fluctuations could deteriorate the product quality especially in the falling rate period when the sample could not absorb 100% level of microwave power. During both drying modes, further temperature rise in falling rate period was not observed at MW power density $P = 1.988$ W/g (PL = 20%) and below. The reason was due to the convective cooling effect of air stream which balanced the absorbed power of sample.

The overall temperature during cycle-controlled drying was slightly higher than that during phase-controlled, which can be explained by that 100% rated power produced intensive mass transfer driving force, and as a result, an enhanced temperature was induced.

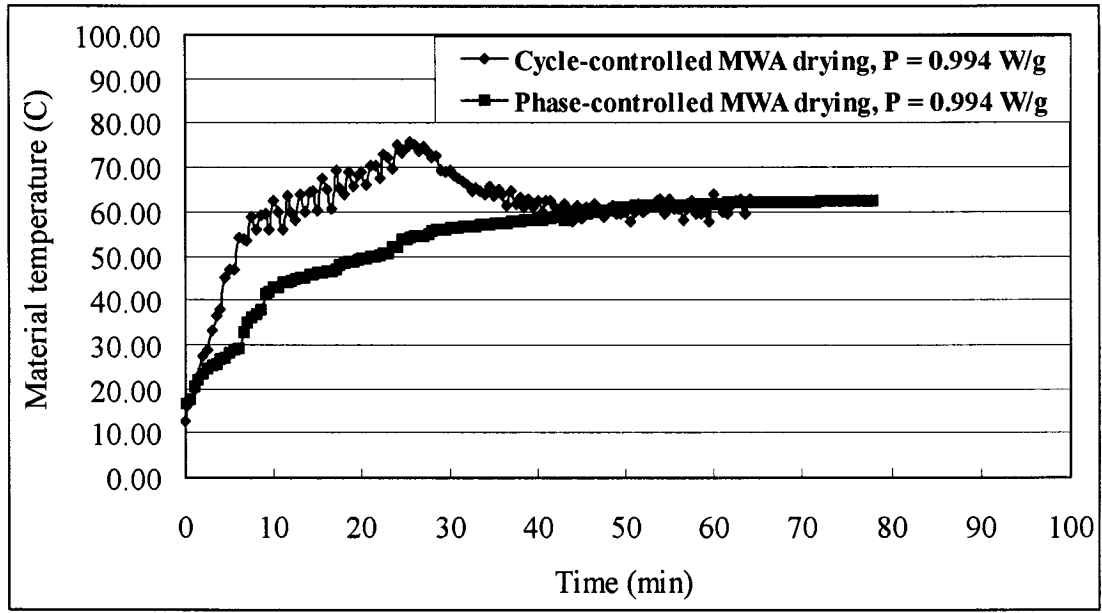


Figure 4.13 Material temperature during drying with power density of 0.994W/g, air temperature at 25°C and air velocity at 0.5m/s

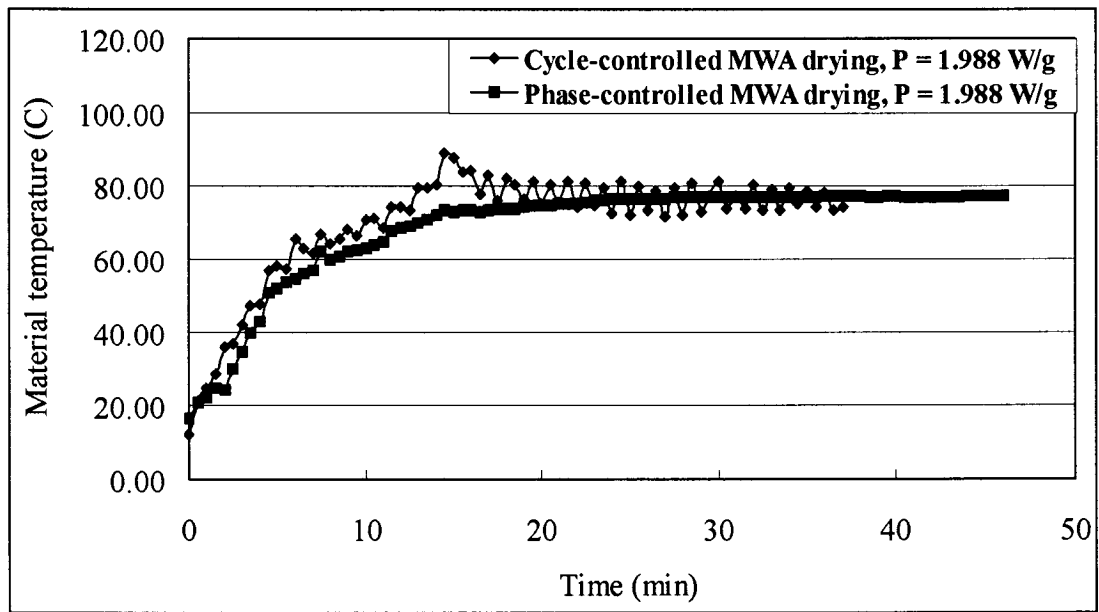


Figure 4.14 Material temperature during drying with power density of 1.988W/g, air temperature at 25°C and air velocity at 0.5m/s

4.4 Quality Evaluation

4.4.1 Rehydration Capacity

Rehydration capacity is an important parameter to evaluate the quality of dried products. Rehydration will be maximized when cellular and structural changes during drying process are minimized (Okas et al. 1992). In this study, potatoes dried by the two different drying modes were studied for rehydration analysis. The rehydration capacity was expressed as a percentage of water gain calculated from the difference in sample mass from before and after rehydration. Table 4.2 shows the results.

Table 4.2 Rehydration capacity of dried potato sample

Power density, W/g	Air velocity, m/s	MWA drying mode	Water gain, %
0.994	0.5	Phase-controlled	195.83 ^a
		Cycle-controlled	179.36 ^b
	1.5	Phase-controlled	243.72 ^c
		Cycle-controlled	213.36 ^d
1.988	0.5	Phase-controlled	168.28 ^b
		Cycle-controlled	125.89 ^e
	1.5	Phase-controlled	196.23 ^a
		Cycle-controlled	181.84 ^b

Superscripts a,b,c,d,e: Values with same superscripts are not significantly different.

The data exhibited the maximum water gain, 243.72%, occurring during phase-controlled MWA drying at $P = 0.994\text{W/g}$ and $V_{\text{air}} = 1.5\text{m/s}$; while the minimum water gain, 125.89%, during cycle-controlled MWA drying at $P = 1.988\text{W/g}$ and $V_{\text{air}} = 0.5\text{m/s}$. At same power density and air velocity, potato samples dried during phase-controlled MWA drying displayed higher rehydration capacity than those dried

during cycle-controlled MWA drying. This might be due to the milder drying process such that less cellular and structural changes happened during phase-controlled MWA drying. At the same air velocity and drying mode, water gains were improved at $P = 0.994\text{W/g}$ compared to those at $P = 1.988\text{W/g}$ implied the latter was still too high for potato drying and was evidenced by more burning sample cubes. At the same power density and drying mode, rehydration properties were benefited from air convective cooling which which are clearly shown in the data.

4.4.2 Colour Analysis

The colour of dried products is also an important attribute for quality assessment. The results of colour measurement during different drying modes, power densities, and air velocities are presented in Table 4.3. Statistical analysis showed that there were no differences in the three colour parameters (L^* , a^* , b^*) between the two drying modes. Also the changes in two colour parameters (a^* , b^*) were independent on the MW power densities and the air velocities.

The colour of the products dried at $P = 0.994\text{W/g}$ and $V_{\text{air}} = 1.5\text{m/s}$ was significantly lighter (higher in L^* value) than the colour of the products dried at $P = 1.988\text{W/g}$ (either $V_{\text{air}} = 0.5$ or 1.5m/s), which implied that the sample temperature was the dominant parameter for colour change during current drying studies.

4.4.3 Sensory Evaluation

Sensory is another essential attribute to appraise quality of dried products. In this study, a panel of six untrained judges was asked to assess for visual appearance, taste, and textural consistency; which were expressed by unsatisfactory, poor, neutral, good, and satisfactory, respectively. The evaluation by judges is presented in Table 4.4. The poor and neutral visual appearances were due to the burning of potato cubes. The rating of good for taste attribute was noted in all treatments. It seems the air velocity favored the

textural consistency which was confirmed by the good results in all $V_{\text{air}} = 1.5$ m/s cases. Overall, the results of sensory evaluation show no differences attributable to different drying modes.

Table 4.3 Colour parameters of dried potato sample

Power density, W/g	Air velocity, m/s	MWA drying mode	L*	a*	b*
0.994	0.5	Phase-controlled	62.74 ^{a,b}	-0.14 ^a	+11.96 ^a
		Cycle-controlled	60.58 ^{a,b}	+1.21 ^a	+10.32 ^a
	1.5	Phase-controlled	64.95 ^a	-0.13 ^a	+10.39 ^a
		Cycle-controlled	64.42 ^a	+0.42 ^a	+12.29 ^a
1.988	0.5	Phase-controlled	57.48 ^b	+1.29 ^a	+12.00 ^a
		Cycle-controlled	55.07 ^b	+1.69 ^a	+12.21 ^a
	1.5	Phase-controlled	58.24 ^b	+0.47 ^a	+12.77 ^a
		Cycle-controlled	58.36 ^b	-0.96 ^a	+11.18 ^a

Superscripts a,b: Values with same superscripts are not significantly different.

Table 4.4 Sensory evaluation of dried potato sample

Power density, W/g	Air velocity, m/s	MWA drying mode	Visual appearance	Taste	Textural consistency
0.994	0.5	Phase-controlled	Neutral	Good	Neutral
		Cycle-controlled	Neutral	Good	Neutral
	1.5	Phase-controlled	Good	Good	Good
		Cycle-controlled	Good	Good	Good
1.988	0.5	Phase-controlled	Poor	Good	Neutral
		Cycle-controlled	Poor	Good	Neutral
	1.5	Phase-controlled	Neutral	Good	Good
		Cycle-controlled	Neutral	Good	Good

CHAPTER V. SUMMARY, CONCLUSIONS AND RECOMMENDATIONS

5.1 Summary and Conclusions

The principle objective of this study was to evaluate the effects of two different input electrical power control methods, phase control and cycle control, on the microwave/air drying process. A phase-controlled electrical power regulator was designed, built, and connected in series with the electrical circuit of an existing domestic microwave oven. The original power control in the microwave oven was realized by a cycle-controlled power regulator. With the addition of the phase-controlled power regulator, the input electrical power could be either cycle-controlled or phase-controlled. The existing domestic microwave oven was also modified such that combined microwave and convectional drying can be accommodated. The system performance was evaluated. The effects of phase-controlled and cycle-controlled input electrical power were evaluated through combined microwave and convective drying of potato samples. This study leads to following conclusions:

- The proposed triac power controller could be successfully used for quasi-continuous (fast-switching) power regulation with maximum power efficiency.
- Factors that should be taken into account in the design of a triac phase controller included (1) load characteristics and selection of thyristors, (2) triggering strategy, (3) transient current and voltage, (4) extent of current and voltage, and (5) dissipation of heat generated in the unit by providing suitable cooling method.
- In the new developed microwave/air drying unit, the input electrical power to magnetron could be either cycle-controlled or phase-controlled. Both strategies are achievable.
- The effects of different power control methods (different patterns of input electrical voltage waveforms) on drying kinetics and product qualities were different. In both

drying modes, the drying time increased with the decrease of microwave power density and the increase of air velocity.

- During microwave/air drying of potatoes, the drying rates of cycle-controlled drying are significantly higher than those of phase-controlled drying. In terms of rehydration capacity the phase-controlled drying mode demonstrated its advantages. The product colour and sensory attributes were independent of the power control methods. Sample temperature had negative effect on the colour while air velocity increased the textural consistency.
- More accurate temperature control could be realized using phase control method compared to cycle control method. This is attributable to product temperature which varied a lot and corresponded to ON and OFF of the duty cycles in cycle-controlled drying. It is also reasonable to expect higher power efficiency using phase control and cycle control than that using resistive control, because the latter process always consumes power at the full capacity.
- The benefits of air cooling were clarified because no further product temperature rose during falling drying rate periods. But the disadvantage is attributable to more energy that is being consumed.
- At MW power density $P = 2.982 \text{ W/g}$ ($PL = 30\%$) and above, the product had serious burnt spots due to higher product temperature which was over 100°C before drying process finished.
- The degradation of output microwave power was observed by calorimetric measurements, the main reason might be due to the aging of the magnetron and not the overheating of the filament.
- The nonuniform distribution of microwave field in the existing microwave oven was confirmed.

5.2 Recommendations

Further studies could be conducted based on the following:

- Power control of three-phase AC power supplies – The current study was concentrated on the control of single-phase AC power supply to a microwave oven. In many industrial applications the electrical power supply to microwave processing equipment are three-phase. There may be a need to develop three-phase AC input power regulator to adjust the output microwave power.
- Microwave electromagnetic waveform control – The current study applied an indirect strategy to control the microwave power by varying the input electrical power. The microwave power could be directly controlled by regulating the microwave electromagnetic waveform.
- Magnetic field control inside magnetron – Microwave power could be changed by adjusting the magnetic field strength inside the magnetron. In such cases an electromagnet should be introduced.
- Introduction of multiple magnetrons and cavities – Because of the nonuniform distribution of microwave field in a single magnetron cavity, the development of the apparatus which can accommodate multiple magnetrons and cavities is needed.

REFERENCES

- Andres, A., C. Bilbao, P. Fito. 2004. Drying kinetics of apple cylinders under combined hot air-microwave dehydration. *Journal of Food Engineering* 63:71-78.
- ASAE. 1991. ASAE standards. American Society of Agricultural Engineers. St. Joseph, USA.
- Beke, J., A. S. Mujumdar and M. Giroux. 1997. Some fundamental attributes of corn and potato drying in microwave fields. *Drying Technology*, 15(2):539-554.
- Bessarabov, A., V. Shimichev and N. Menshutina. 1999. Microwave drying of multicomponent sols. *Drying Technology*, 17(3): 379-394.
- Bows, J. R., J. T. Mullin, L. Barratt, R. A. Blindt and J. F. Crilly. 1997. Apparatus and method for heating objects with microwaves. Patent EP 792085.
- Bows, J. R., M. L. Partrick, R. Janes, A. C. R. Metaxas and D. C. Dibben. 1999. Microwave phase control heating. *International Journal of Food Science and Technology*, 34: 295-304.
- Carter, R. G. 1990. *Electromagnetic waves: microwave components and devices*. Chapman and Hall, London, UK.
- Chambers, D., C. Scapellati. 1994. New high frequency high voltage power supplies for microwave heating applications. Proceedings of 29th Microwave Power Symposium (IMPI), Chicago, Illinois, July, 1994.

Chen, D. D., Singh, R. K., Haghighi, K. and Nelson, P. E. 1993. Finite element analysis of temperature distribution in microwave cylindrical potato tissue. *Journal of Food Engineering*, 18:351-368.

Cohen, J. S., J. A. Ayoub, T. C. Yang. 1992. A comparison of conventional and microwave augmented freeze-drying of peas. In: *Drying'92*, Mujumdar, A. S. ed., Elsevier Science Publishers B. V., San Diego, USA, pp585-594.

Copson, D. A. 1975. *Microwave heating*. Avi Pub Co., Westport, USA.

Costa, L.M., F. V. Silva, S. T. Gouveia, A. R. A. Nogueira, and J. A. Nobrega. 2001. Focused microwave-assisted acid digestion of oils: an evaluation of the residual carbon content. *Spectrochimica Acta Part B* 56: 1981-1985.

Datta, S. K. 1985. *Power electronics and controls*. Reston Publishing Company, Inc., Reston, USA.

Davis, C., S. Neill, P. Raj. 1997. Microwave fixation of rabies specimens for fluorescent antibody testing. *Journal of Virological Methods*, 68:177-182.

Decareau, R. V. 1985. *Microwave in the food processing industry*. Academic Press, Orlando, USA.

Decareau, R. V. and R. A. Peterson. 1986. *Microwave processing and engineering*. VCH, Chichester, UK.

Drouzas, A. E. and H. Schubert. 1996. *Microwave application in vacuum drying of fruits*.

Journal of Food Engineering, 28: 203-209.

Drouzas, A. E., E. Tsami and G. D. Saravacos. 1999. Microwave/vacuum drying of model fruit gels. Journal of Food Engineering, 39: 117-122.

Finney, D. 1980. The power thyristor and its applications. McGraw-Hill Book Company (UK) Limited, Maidenhead, UK.

Fisher, M. J. 1991. Power electronics. PWS-Kent Publishing Company, Boston, USA.

Fuller, A. J. B. 1990. Microwaves: an introduction to microwave theory and techniques. Pergamon Press, Oxford, UK.

Fritz, K. 1988. System for heating objects with microwaves. Patent US 4775770.

Gallawa, J. C. 1999. Complete microwave service handbook: operation, maintenance, troubleshooting, and repair. Prentice Hall College Div, Englewood Cliffs, USA.

Gardiol, F. 1984. Introduction to microwaves. Artech House, Dedham, USA.

Glouannec, P., D. Lecharpentier and H. Noel. 2002. Experimental survey on the combination of radiating infrared and microwave sources for the drying of porous material. Applied Thermal Engineering, 22:1689-1703.

Heumann, K. 1985. Basic principles of power electronics. Springer-Verlag, Berlin, Germany.

Ishii, T. K. 1990. Practical microwave electron devices. Academic Press, San Diego, USA.

Jia, X. 1992. Mathematical and experimental modeling of heat pump assisted microwave drying. Ph. D. Thesis, Department of Mechanical Engineering, The University of Queensland, Queensland, Australia.

Jones, P. L. and A. Rowley. 1996. Dielectric drying. *Drying Technology*, 14(5): 1063-1098.

Jumah, R. Y., A. S. Mujumdar and G. S. V. Raghavan. 1995. Control of industrial dryers. In: *Handbook of industrial drying (second edition)*, Mujumdar, A. S. ed., Marcel Dekker, Inc., New York, USA, pp1343-1368.

Jumah, R. Y. and G. S. V. Raghavan. 2001. Analysis of heat and mass transfer during combined microwave-convective spouted-bed drying. *Drying Technology*, 19(3&4): 485-506.

Khrasisheh, M. A. M., T. J. R. Cooper and T. R. A. Magee. 1997. Microwave and air drying I: fundamental considerations and assumptions for the simplified thermal calculations of volumetric power absorption. *Journal of Food Engineering* 33: 201-219.

Khrasisheh, M. A. M., W. A. M. McMinn, T. R. A. Magee. 2000. A multiple regression approach to the combined microwave and air drying process. *Journal of Food Engineering* 43:243-250.

Kingston, H. M. and L. B. Jassie. 1988a. Monitoring and predicting parameters in

microwave dissolution. In: Introduction to microwave sample preparation, Kingston, H. M. and L. B. Jassie ed., American Chemical Society, Washington, USA, pp93-154.

Kingston, H. M. and L. B. Jassie. 1988b. Safety guidelines for microwave systems in the analytical laboratory. In: Introduction to microwave sample preparation, Kingston, H. M. and L. B. Jassie ed., American Chemical Society, Washington, USA, pp231-243.

Kok, L. P., P. E. Visser and M. E. Boon. 1994. Programming the microwave oven. *Journal of Neuroscience Methods* 55:119-124.

Krein, P. 2001. Introduction. In: *Power electronics handbook*, Rashid, M. H. ed., Academic Press, San Diego, USA, pp1-12.

Kudra, T. and A. S. Mujumdar. 2002. *Advanced drying technologies*. Marcel Dekker, Inc., New York, USA.

Laster, C. 1981. *SCRs and related thyristor devices*. Howard W. Sams & Co., Inc., Indianapolis, USA.

Lin, T. M., T. D. Durance and C. H. Scaman. 1998. Characterization of vacuum microwave, air and freeze dried carrot slices. *Food Research International*, 31(2): 111-117.

Litvin, S., C. H. Mannheim and J. Miltz. 1998. Dehydration of carrots by a combination of freeze drying, microwave heating and air or vacuum drying. *Journal of Food Engineering*, 36:103-111.

Login, G. R., N. Tanda, and A. M. Dvorak. 1996. Calibrating and standardizing microwave ovens for microwave-accelerated specimen preparation. *Cell Vision*, 3:172-179.

Lu, L., J. Tang and X. Ran. 1999. Temperature and moisture changes during microwave drying of sliced food. *Drying Technology*, 17(3):413-432.

Maskan, M. 2001. Kinetics of color change of kiwifruits during hot air and microwave drying. *Journal of Food Engineering*, 48:169-175.

Mazda, F. F. 1993. *Power electronics handbook: components, circuits and applications*. Butterworths, Oxford, UK.

McGuire, R. G. 1992. Reporting of objective color measurements. *Hortscience*, 27(12):1254-1255.

Meredith, R. 1998. *Engineers' handbook of industrial microwave heating*. The Institution of Electrical Engineers, London, UK.

Metaxas, A. C. and R. J. Meredith. 1983. *Industrial microwave heating*. Peter Peregrinus, London, UK.

Mujumdar, A.S. 2003. Drying of biotechnological products: current status and new developments. In: *Food science and food technology*, Gutierrez-Lopez, G. F. and G.V. Barbosa-Canovas ed., CRC Press, Boca Raton, USA, pp267-277.

Neas, E. D. and M. J. Collins. 1988. *Microwave heating: theoretical concepts and*

equipment design. In: Introduction to microwave sample preparation, Kingston, H. M. and L. B. Jassie ed., American Chemical Society, Washington, USA, pp7-32.

Pandit, R. B. and S. Prasad. 2003. Finite element analysis of microwave heating of potato – transit temperature profiles. *Journal of Food Engineering* , 60:193-202.

Pearman, R. A. 1980. Power electronics: solid state motor control. Reston Publishing Company, Inc., Reston, USA.

Prabhanjan, D. G., H. S. Ramaswamy and G. S. V. Raghavan. 1995. Microwave-assisted convective air drying of thin layer carrots. *Journal of Food Engineering*, 25: 283-293.

Prothon, F., L. M. Ahrne, T. Funebo, S. Kidman, M. Langton, and I. Sjöholm. 2001. Effects of combined osmotic and microwave dehydration of apple on texture, microstructure and rehydration characteristics. *Lebensm. Wiss. U. Technol.*, 34: 95-101.

Puacz, W. and W. Szahun. 1996. Application of microwave energy to cleavage of sulfur bonds in the S₈ ring in the simplest amide solvents. *Microchemical Journal* 53:446-453.

Raghavan, G. S. V., P. Alvo and U. S. Shivare. 1993. Microwave drying of cereal grain: advantages and limitations. *Postharvest News and Information*, 4(3): 79N-83N.

Raghavan, G. S. V. and A. M. Silveira. (2001) Shrinkage characteristics of strawberries osmotically dehydrated in combination with microwave drying. *Drying Technology*, 19(2):405-414.

Ramshaw, R. 1975. Power electronics: thyristor controlled power for electric motors. Chapman and Hall, London, UK.

Ramaawamy, H., F. R. Van De Voort, G. S. V. Raghavan, D. Lightfoot and G. Timbers. 1991. Feed-back temperature control system for microwave ovens using a shielded thermocouple. *Journal of Food Science*, 56(2): 550-555.

Rashid, M. H. 1988. Power electronics: circuits, devices, and applications. Prentice Hall, Englewood Cliffs, USA.

Ren, G., F. Chen. 1998. Drying of American ginseng (*Panax quinquefolium*) roots by microwave-hot air combination. *Journal of Food Engineering*, 35:433-443.

Roussy, G. and J. A. Pearce. 1995. Foundations and industrial applications of microwaves and radio frequency fields: physical and chemical processes. John Wiley & Sons, Chichester, UK.

Sanga, E. C. M., A. S. Mujumdar and G. S. V. Raghavan. 2000. Microwave drying: principles and applications. In: *Developments in drying (I): food dehydration*, Mujumdar, A. S. and S. Suvachittanont ed., Kasetsart University Press, Bangkok, Thailand, pp112-141.

Sanga, E. C. M., A. S. Mujumdar and G. S. V. Raghavan. 2001. Experimental and numerical analysis of intermittent microwave-convection drying. In: *Proceedings of Asia-Australia Drying Conference*, Ramli, E. W. ed., Institution of Chemical Engineerings Publication, Malaysia, pp203-215.

Sanga, E. C. M. 2002. Microwave assisted drying of composite materials: modeling and experimental validation. Ph. D. Thesis, Department of Chemical Engineering, McGill University, Montreal, Canada.

Schiffmann, R. F. 1987. Microwave and dielectric drying. In: Handbook of industrial drying, Mujumdar, A. S. ed., Marcel Dekker, Inc., New York, USA.

Schiffmann, R. F. 1995. Microwave and dielectric drying. In: Handbook of industrial drying (second edition), Mujumdar, A. S. ed., Marcel Dekker, Inc., New York, USA, pp345-372.

Scott, A. W. 1993. Understanding microwaves. John Wiley & Sons, Inc., New York, USA.

Sharma, G. P. and S. Prasad. 2001 Drying of garlic (*Allium sativum*) cloves by microwave – hot air combination. Journal of Food Engineering, 50:99-105.

Shepherd, W., L. N. Hulley and D. T. W. Liang. 1995. Power electronics and motor control. Cambridge University Press, Cambridge, UK.

Shivhare, U. S., G. S. V. Raghavan and R. G. Bosisio. 1991. Drying of corn using variable microwave power with a surface wave applicator. Journal of Microwave Power and Electromagnetic Energy, 26(1): 38-44.

Shivhare, U. S., G. S. V. Raghavan, R. G. Bosisio and A. S. Mujumdar. 1992a. Microwave drying of corn III: constant power, intermittent operation. Transactions of the ASAE, 35(3): 959-962.

Shivhare, U. S., G. S. V. Raghavan and R. G. Bosisio. 1992b. Microwave drying of corn II: constant power, constant operation. *Transactions of the ASAE*, 35(3): 951-957.

St-Denis, E. 1998. Performance optimization of a multi-slotted waveguide for microwave processing applications. MSc. Thesis, Department of Agricultural and Biosystems Engineering, McGill University, Montreal, Canada.

Sun, G., W. Li, F. Wang, G. Yang, F. Sun. 2000. The digital continuous power control of high-power microwave source. *Acta Scientiarum Naturalium Universitatis Nankaiensis*, 33:116-118.

Sunjka, P. S. 2003. Microwave/vacuum and osmotic drying of cranberries. MSc. Thesis, Department of Agricultural and Biosystems Engineering, McGill University, Montreal, Canada.

Teccor Electronics. 2003. Thyristor product catalog, website, <http://www.teccor.com>.

Trzynadlowski, A. M. 1998. Introduction to modern power electronics. John Wiley & Sons, Inc., New York, USA.

Tulasidas, T. N. 1994. Combined convective and microwave drying of grapes. Ph. D. Thesis, Department of Agricultural Engineering, McGill University, Montreal, Canada.

Tulasidas, T. N., G. S. V. Raghavan and A. S. Mujumdar. 1995. Microwave drying of grapes in a single mode cavity at 2450 MHz – I: drying kinetics; II: Quality and energy aspects. *Drying Technology*, 13 (8&9): 1949-1992.

Van Zante, H. J. 1973. The microwave oven. Houghton Mifflin, Boston, USA.

Venkatachalapathy, K. 1998. Combined osmotic and microwave drying of strawberries and blueberries. Ph. D. Thesis, Department of Agricultural and Biosystems Engineering, McGill University, Montreal, Canada.

Venkatachalapathy, K. and G. S. V. Raghavan. 2000. Microwave drying of whole, sliced and pureed strawberries. *Agricultural Engineering Journal*, 9(1): 29 - 39.

Williams, B. W. 1992. Power electronics: devices, drivers, applications, and passive components. McGraw-Hill, New York, USA.

Yongsawatdigul, J. and S. Gunasekaran. 1996. Microwave vacuum drying of cranberries: Part I: Energy use and efficiency. Part II: Quality evaluation. *Journal of Food Processing and Preservation*, 20: 121-143.

Zhou, L., V. M. Puri and R. C. Anantheswaran. 1994. Effect of temperature gradient on moisture migration during microwave heating. *Drying Technology*, 12(4): 777-798.